Received: 17 June 2022 | Revised: 20 December 2022 | Accepted: 25 December 2022

DOI: 10.1111/bre.12749

RESEARCH ARTICLE

Basin Research | IAS EAGE | WILEY

Tectonostratigraphic controls on pore fluid pressure distribution across the Taranaki Basin, New Zealand

Sean R. O'Neill[1] | **Stuart J. Jones**[1] | **Peter J. J. Kamp**[2]

[1]Department of Earth Sciences, Durham University, Durham, UK

[2]School of Science, University of Waikato, Hamilton, New Zealand

Correspondence
Sean R. O'Neill, Department of Earth Sciences, Durham University, Durham DH1 3LE UK.
Email: sean.oneill@durham.ac.uk

Funding information
Ministry for Business Innovation and Employment, Grant/Award Number: CONT-42907-EMTR-UOW; Natural Environment Research Council, Grant/Award Number: NEM00578X/1

Abstract

Significant variations in pore pressure across the Taranaki Basin, New Zealand, are attributed to changes in lithofacies and structure, usefully illustrated in terms of ten areas that we term geopressure provinces, each displaying individual pore pressure trends. Cretaceous to Early Miocene formations in different parts of the basin can be either normally pressured (near or at hydrostatic) or significantly overpressured (up to 28 MPa) at the same depth. Variations in Eocene–Oligocene facies types and thicknesses both within and between geopressure provinces provide first-order control on the magnitude, distribution and maintenance of overpressure across the basin. Examples of hydraulic compartmentalisation due to sealing faults and stratigraphic architecture are identified within the basin. Deep pore pressure transitions are sealed by diagenetic, structural or stratigraphic mechanisms in different places and are associated with an increase in mudrock volume (reduced permeability) or gas generation. Thus, pore pressure distribution in the Taranaki Basin is controlled by a combination of sediment loading, lithofacies variations, fault zone permeability and structural architecture. This work represents an appraisal of the pore pressure distribution across the whole of a multiphase structurally complex basin, and the approach taken provides a framework for better understanding the distribution of pore fluid pressures and pore fluid migration in other sedimentary basins.

KEYWORDS

compartmentalisation, lithofacies, overpressure, pore pressure, tectonostratigraphy

1 | INTRODUCTION

Pore fluid pressure distribution within a sedimentary basin is controlled by a combination of factors, including stratigraphic stacking, lithofacies distribution, fault zone permeability, sedimentation rate, diagenesis, petroleum generation and structural evolution. Basins with an initial rift phase coupled with high sedimentation rates often display pore fluid pressures above hydrostatic, but subsequent structural shortening can drastically alter the initial distribution of pore fluid pressure. Pore fluid pressure in excess of the hydrostatic gradient (overpressure) has been shown in several sedimentary basins to increase basinward (e.g. Javanshir et al., 2015; Tingay et al., 2005; Van Balen & Cloetingh, 1994; Zoccarato et al., 2018) due to a gradual reduction in sand-to-mudrock ratio (net-to-gross), resulting in decreasing hydraulic connectivity and permeability (Harrison & Summa, 1991) and an increased likelihood of permeable (sandstone) beds maintaining overpressure. The effectiveness of mudrock in maintaining overpressure also determines the nature of pressure transition zones within stratigraphic sections (Swarbrick & Osborne, 1996). Reactivation of initial normal faults can lead to hydraulic compartmentalisation and the generation of pressure cells within geopressure provinces, as demonstrated in the North Sea Basin (Borge, 2002; Darby et al., 1996).

Processes acting on a basin to microscopic scale define both the maintenance and flow of excess pressure within a sedimentary basin. Knowledge about the distribution of pore pressure within a permeable formation together with its relationship to overpressure maintaining facies (e.g. mudrock) is a useful means for investigating lateral fluid flow and regional migration pathways (e.g. Iliffe et al., 1999; Javanshir et al., 2015; O'Connor & Swarbrick, 2008; Robertson et al., 2013). Excess pressure is prone to re-equilibrate to hydrostatic pressure within an inclined reservoir or into shallower reservoirs by fluid migration through faults or fractures (Tingay et al., 2007; Yardley & Swarbrick, 2000). Fault-controlled fluid overpressure compartmentalisation has been identified in sedimentary basins worldwide, through cataclasis in fault zones, shale gouge or diagenetic alteration (Darby et al., 1996; Prada et al., 2018; Richards et al., 2010; Wonham et al., 2010). Hydraulic compartmentalisation of pore fluids occurs when flow is prevented from migrating across 'sealed' boundaries, resulting in the segregation of pore fluids into separate fluid/pressure compartments (Jolley et al., 2010).

Previous investigations of pore fluid overpressure at basin scales tend to have restricted geographical resolution due to the limited spatial availability of pore fluid pressure data (e.g. Drews et al., 2018; Morley et al., 2008; Shi et al., 2013; van Ruth et al., 2000). Studies focused on a sub-basin scale (He & Middleton, 2002; Robertson et al., 2013; Williamson, 1995; Xie et al., 2001) do highlight spatial variations in pore fluid pressure but by their nature are not basin-wide investigations. The Taranaki Basin, New Zealand, is known to have significant spatial variations in pore fluid pressure (Webster et al., 2011), and it has a wealth of high-quality data across the whole of the basin, thereby allowing for high spatial resolution of pore fluid pressure. This study, therefore, provides a useful pore fluid pressure analogue for tectonically active and structurally and stratigraphically partitioned basins globally.

Highlights

- Ten new geopressure provinces are identified across Taranaki Basin.
- Lithofacies type and mudrock thickness control the overpressure distribution and magnitude.
- Pore pressure depth transitions are controlled by diagenetic, structural and stratigraphic mechanisms.
- Disequilibrium compaction controls the maintenance of overpressure.

Pore pressure distribution within the Taranaki Basin (Figure 1) has previously been defined using a discrete overpressure range approach (e.g. Webster et al., 2011), which resulted in the identification of three overpressure zones, defined partly by depth and partly by stratigraphic variations: a near-hydrostatic interval (Zone A), which extends from the surface to varying depths in different parts of the basin; an underlying overpressured interval (Zone B) of ca. 7.6 MPa (12.8 MPa/km, 10.9 ppg), which extends from ca. 2500 m to ca. 4300 m; and a third interval (Zone C) of >14.5 MPa (14.4 MPa/km, 12.3 ppg) beneath zones A and B in some parts of the basin. The Oligocene Otaraoa Formation (Figure 2), a bathyal calcareous mudrock, was identified as the principal top seal between hydrostatic Zone A and deeper variably overpressured zones. The Otaraoa formation together with the underlying Turi formation is considered to be the formations where overpressure (low vertical effective stress) is maintained in the basin through disequilibrium compaction (Webster et al., 2011). Horizontal stresses can also contribute to the maintenance of overpressures (Burgreen-Chan et al., 2016), but as the Taranaki Basin is now situated in a back-arc extensional setting (King & Thrasher, 1996), these stresses are no longer being applied, therefore any previously maintained excess pressure will have dissipated.

This work tests the Webster et al. (2011) model through the analysis of a more comprehensive set of pressure data for wells that have become open file (Figure 3a,b) since the Webster et al. (2011) study was undertaken. Our

FIGURE 1 Map of the Taranaki Basin and ten numbered geopressure provinces displaying different pore pressure profiles due to differences in structure, lithofacies and bathymetry. Only key wells are shown in this figure. 1. Southern Taranaki Inversion Zone (orange); 2. Central Taranaki (purple); 3. Manaia Anticline (brown); 4. Central Taranaki Peninsula (red); 5. Tarata Thrust Zone (turquoise); 6. Patea-Whanganui Coast (pink); 7. Manganui Platform (lilac); 8. Northern Graben (grey); 9. Oligocene sandstones (yellow), 10. Western Platform (green). See Figure 4a for line A–A′; Figure 4b for line B–B′; Figure 8 for line C–C′; Figure 6 for line D–D′; and Figure 9 for line E–E′ (bathymetry after Mitchell et al., 2012).

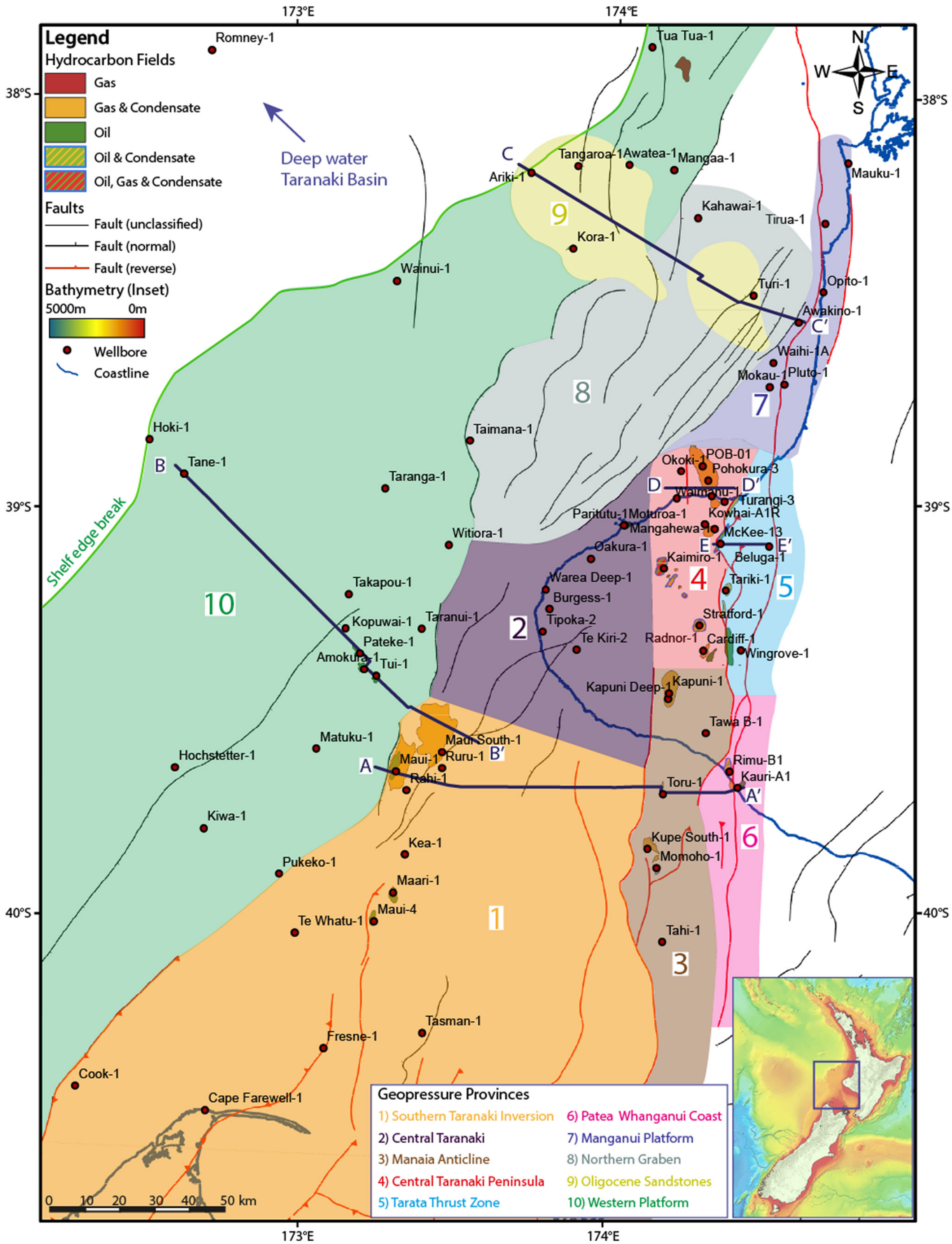

additional datasets have demonstrated that pore pressure distribution is more complex than the three semi-stratigraphic overpressure zones model.

In this study, differences in the distribution of sedimentary facies, stratigraphic architecture and structural development across the Taranaki Basin, are found to define

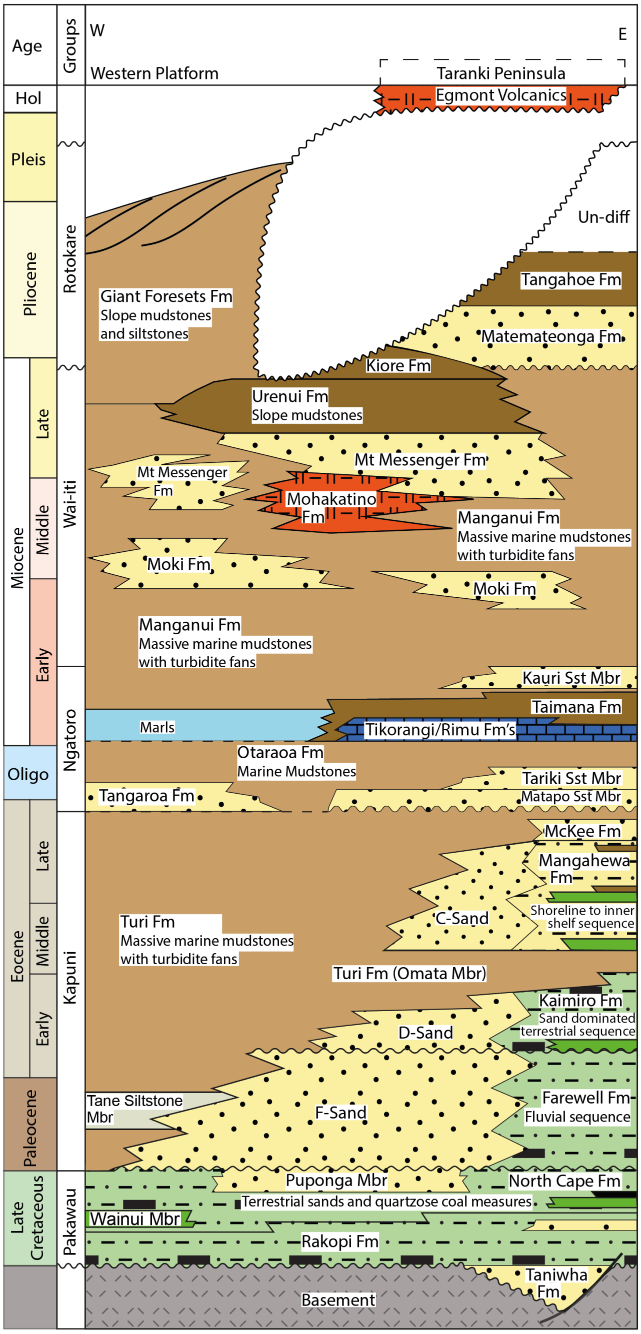

FIGURE 2 Subsurface stratigraphy of the Taranaki Basin east to west from the Taranaki peninsula to the Western Platform (modified from King & Thrasher, 1996).

areas that we term geopressure provinces, which our data show to have characteristic pore pressure distributions with depth that may influence regional fluid flow pathways. Consideration of the distribution of pore pressure across a whole basin, particularly one where sedimentation continued during successive phases of deformation, may be an approach that can be applied to other basins to understand compartmentalisation of pore fluid pressure and related fluid migration. This study highlights the great value of pore fluid pressure data and implications for structural geology, facies analysis, geohazards, gas storage, drilling operations and regional subsurface fluid flow.

1.1 | Development of the Taranaki Basin—Depositional systems, timing and style of deformation

The Taranaki Basin covers approximately 100,000 km^2 underlying the Taranaki Peninsula and the shelf and continental slope offshore of central-western North Island (Figure 1). It contains an Upper Cretaceous to Quaternary sedimentary fill up to 8 km thick (King & Thrasher, 1996). There is a relatively undeformed block in the northwest known as the Western Platform. A significantly deformed area termed the Eastern Mobile Belt occurs beneath the eastern Taranaki Peninsula.

The sedimentary fill of the Taranaki Basin is illustrated in Figure 2. Full description of the basin fill, related syn-sedimentary structures and the paleogeographic development of the basin are given in King and Thrasher (1996) and Strogen (2011), Strogen, Bland, Nicol, and King (2014) and Strogen et al. (2017). Particularly relevant basin elements for this study are as follows:

1. Early extension (84–57 Ma) and influx of clastic sediments resulted in the accumulation of fluvial sandstone beds and intervening coal measures (Rakopi, North Cape and Farewell formations), including extensive neritic sandstone (F-Sand) (Figure 2).
2. The Eocene section is characterised by fluvial Kaimiro Formation and associated neritic D and C Sand units and McKee Formation shoreface sandstone, with intervening Turi Formation. (Figure 2).
3. During the Late Eocene, normal faults in the vicinity of the Taranaki Peninsula were re-activated as reverse faults forming the Manaia Anticline in the Kapuni and Kupe gas condensate fields (central-southern Peninsula and offshore to the south) (Strogen, Bland, Nicol, & King, 2014; Voggenreiter, 1993).
4. The Early Oligocene (33–29 Ma) section is characterised by unconformity development with mild erosion across central and southern parts of the Taranaki Peninsula (King & Thrasher, 1996; Strogen et al., 2017), whereas, during ca. 29–27 Ma a foredeep developed along the eastern margin of the Taranaki Peninsula (Holt & Stern, 1994; Stern & Davey, 1990; Strogen et al., 2017) due to basement overthrusting on the Taranaki Fault (Kamp et al., 2014; Tripathi & Kamp, 2008). A thick (800 m) calcareous mudstone succession (Otaraoa Formation) then accumulated in the foredeep associated with intervening small submarine fan deposits (Tariki Sandstone Member) (de Bock et al., 1990).

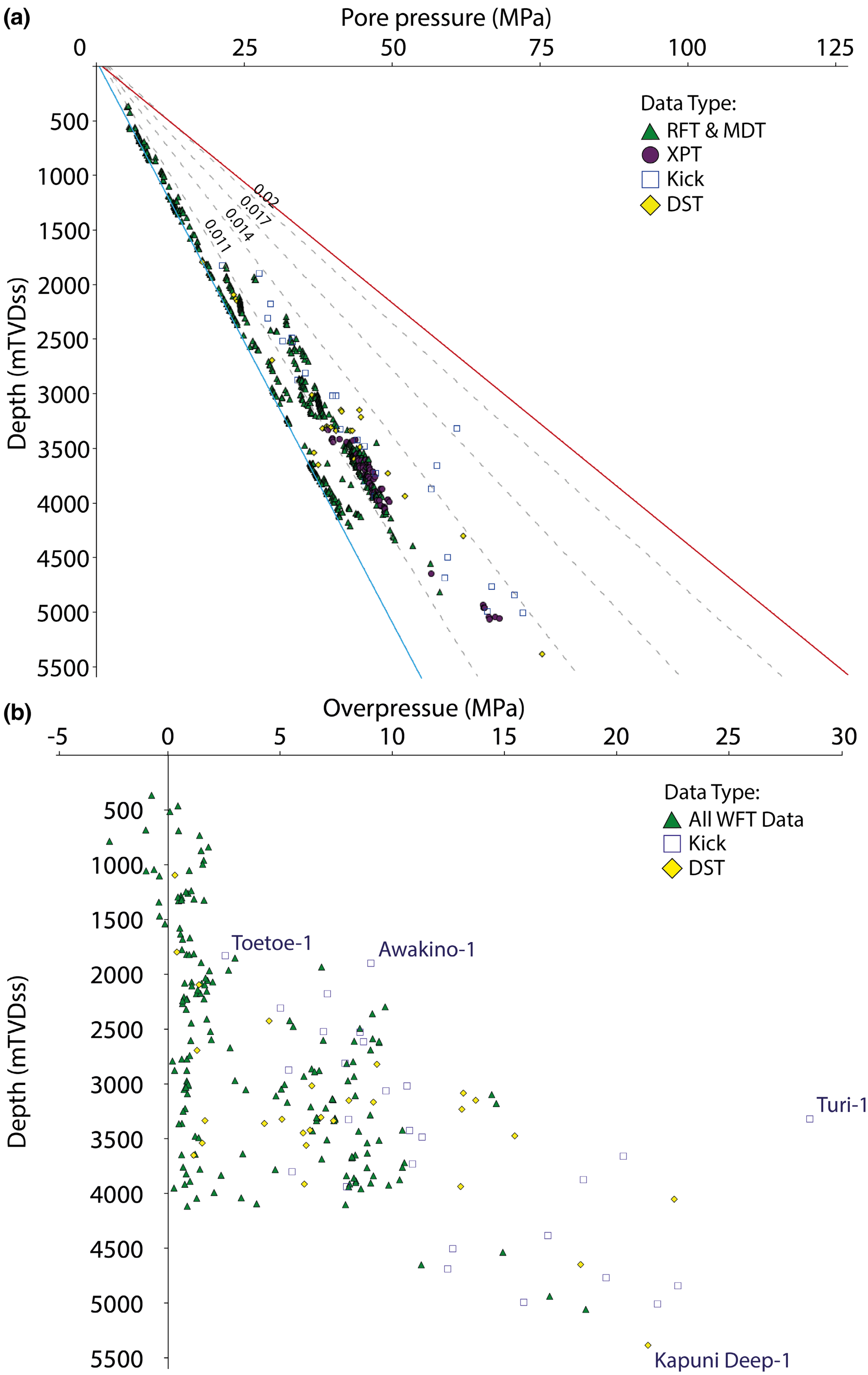

FIGURE 3 (a) Basin-wide plot of formation pore pressure against depth (all WFT data are designated as either good or fair, which stabilise to 0.1 psi over 45 s). DST and kick data are included, but no quality designation is given. (b) Basin-wide plots of overpressure against true vertical depth labelled by data type and annotated with key wells. Most overpressure estimates of more than 13.8 MPa (14.1 MPa/km, 12 ppg) are recorded from kicks and drill stem tests. (Blue line: Hydrostatic pressure; red line: Lithostatic pressure; dashed lines: Pressures gradients in MPa/km).

5. During the latest Oligocene and earliest Miocene (25–22 Ma), bioclastic sediments formed upon a basement high along the eastern basin margin and were eroded and deposited westward into the Taranaki Basin foredeep, forming the Tikorangi Limestone (Hood et al., 2003) (Figure 2).
6. The Early Miocene (22–19 Ma) marked a significant phase of basement overthrusting on the Taranaki Fault (Kamp et al., 2014; Stagpoole & Nicol, 2008) and the accumulation of terrigenous mud in the basin (Manganui Formation). Bathyal mudstone is the main facies in the Neogene section, which also contains amalgamated slope to basin floor channelised sandstone facies and submarine fans (Moki and Mt Messenger formations).
7. In the Eastern Mobile Belt, thin-skinned splayed thrust faults, which display sled-runner geometries rooted into the Taranaki Fault (Tarata Thrust Zone), deformed the Paleogene and E. Miocene succession, forming anticline segments at their terminations.
8. The Late Miocene and Pliocene structure development in the southern Taranaki Basin was characterised by reverse displacement on prior normal faults, forming prominent antiform structures (Crowhurst et al., 2002; Kamp & Green, 1990), the erosion of which helped force progradation of the existing shelf-slope system to the northwest during 11–7 Ma (Masalimova et al., 2016; Sharman et al., 2015), together with sediment being concurrently supplied from the emerging Southern Alps (Tippett & Kamp, 1993).
9. During the Late Miocene—Early Pliocene, an extensional graben formed in the northern Taranaki Basin (Giba et al., 2010), being a significant depocentre for terrigenous sediment accumulation. Subsequently, (3.0–1.6 Ma) a shelf-slope wedge (up to 2 km thick) prograded to the northwest across the northern and central Taranaki Basin, known as the Giant Foresets Formation (Hansen & Kamp, 2004; King & Thrasher, 1996; Mattos et al., 2018; Salazar et al., 2018).

2 | METHODOLOGY

In this study, well pressure depth plots were prepared for 127 wells in the Taranaki Basin, of which 99 contained direct wireline formation tester (WFT) data (RFT, MDT, XPT, FIT and RCI), 23 contained Drill Stem Tests (DST) and 21 contained wellbore kicks. Values of overpressure were calculated using IKON Sciences *RokDoc* software (v.6.3.0.272) and these values were assigned to the correct reservoir unit by referring to composite logs, biostratigraphy and wireline data. The final database comprising >2000 WFT measurements was used to calculate 228 formation overpressure values. Quality control was applied to reject any pressure values that might have been affected by pore pressure drawdown associated with hydrocarbon production in nearby fields. This was achieved through the visualisation of data from the same field (or geopressure province) on a multi-well plot and by comparing the overpressure values, which indicated whether those pressures represent virgin pressure or whether production-related depletion had caused a change in the pressure regime.

All of the WFT and kick data were collected from well completion reports and their associated enclosures, supplied in the 2015 & 2018 New Zealand Petroleum Exploration Data Pack (NZP&M, 2018) (https://data.nzpam.govt.nz/GOLD/system/mainframe.asp). DST data were collected from Leap Energy's New Zealand ArcGIS Geodatabase (Leap Energy, 2014). All the raw pore pressure data included in this study can be found in the supplementary material.

2.1 | Direct pressure measurements

2.1.1 | Quality control of wireline formation testers

Wireline Formation Test (WFT) tools are considered by some workers to be the most reliable and efficient method of acquiring multiple pressure measurements in open-hole conditions (Gunter & Moore, 1987). Obtaining high-quality interpretations from pressure data requires particular attention to be given to data acquisition procedures and interpretation techniques (Gunter & Moore, 1987). Wireline formation tests can be assigned a measure of quality based on their 'build-up plots', depending on whether the tests have reached equilibrium or full build-up with respect to the formation pore fluid pressure. In this study >2000 build-up plots have been analysed and quality values applied to each of the pressure points. Only tests that produced a reading that stabilises to within 0.1 psi (0.0007 MPa) over a 45-second interval have been included in the final data set.

FIGURE 4 Interpreted seismic cross-sections: (a) southern Taranaki Basin from the Patea-Whanganui coast to the Maui high, displaying thrusted 'sled runners' on the eastern basin margin and variations in the thickness of the Oligocene section; (b) from the Maui high across the Western platform to the present-day shelf edge, displaying variations in net-to-gross in the Eocene stratigraphy and associated changes in mudrock pressures (seismic section illustration is modified from Strogen, Bland, Bull, et al., 2014).

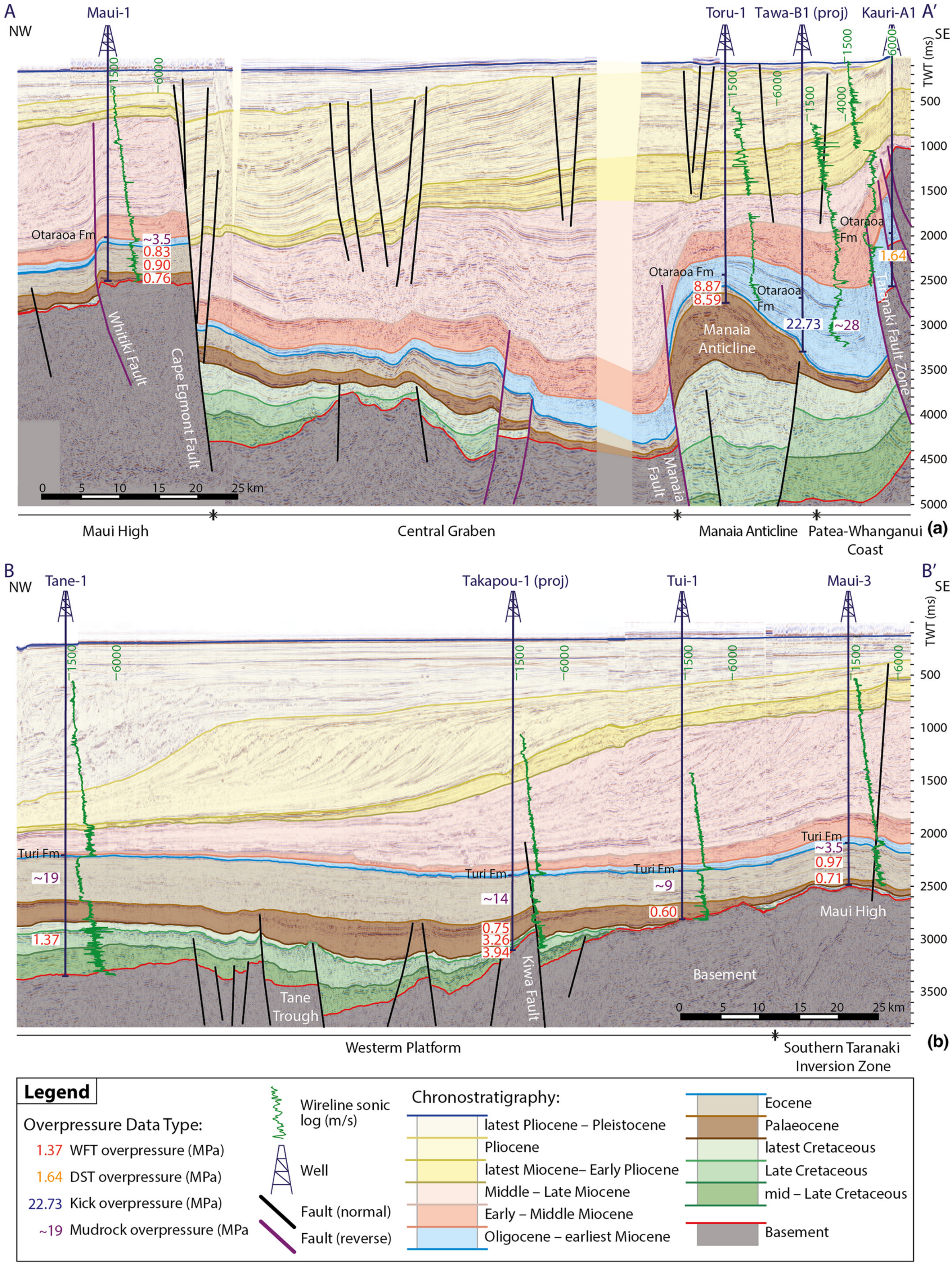
A
NW
Maui-1
Toru-1
Tawa-B1 (proj)
Kauri-A1
A′
SE
TWT (ms)
Otaraoa Fm
~3.5
0.83
0.90
0.76
Whitiki Fault
Cape Egmont Fault
Otaraoa Fm
8.87
8.59
Otaraoa Fm
Manaia Anticline
22.73
~28
Otaraoa Fm
1.64
Taranaki Fault Zone
Manaia Fault
0 5 10 15 20 25 km
Maui High
Central Graben
Manaia Anticline
Patea-Whanganui Coast
(a)
B
NW
Tane-1
Takapou-1 (proj)
Tui-1
Maui-3
B′
SE
TWT (ms)
Turi Fm
~19
1.37
Turi Fm
~14
0.75
3.26
3.94
Turi Fm
~9
0.60
Turi Fm
~3.5
0.97
0.71
Maui High
Basement
Tane Trough
Kiwa Fault
0 5 10 15 20 25 km
Westerm Platform
Southern Taranaki Inversion Zone
(b)
Legend
Overpressure Data Type:
1.37 WFT overpressure (MPa)
1.64 DST overpressure (MPa)
22.73 Kick overpressure (MPa)
~19 Mudrock overpressure (MPa
Wireline sonic log (m/s)
Well
Fault (normal)
Fault (reverse)
Chronostratigraphy:
latest Pliocene – Pleistocene
Pliocene
latest Miocene– Early Pliocene
Middle – Late Miocene
Early – Middle Miocene
Oligocene – earliest Miocene
Eocene
Palaeocene
latest Cretaceous
Late Cretaceous
mid – Late Cretaceous
Basement

Pressure points are designated as 'invalid' when the wireline tool has encountered problems and failed to acquire a representative reading of the formation pressure. The two most commonly encountered problems are a 'tight' formation and 'seal failure'. In a tight test, the formation usually has low permeability and the test is abandoned if it cannot be conducted in a 15–20 min interval. Seal failures occur when the pressure reading probe is not isolated from borehole mud, which results in a rapid pressure build-up to static mud pressure. Also, in low permeability formations, drilling mud can invade the formation and retain some of the excess pressure, which is called 'supercharging', observed when the formation pressure is equivalent to, or higher than, the static mud pressure.

2.1.2 | Drill stem tests

Drill stem tests are typically carried out during drilling when zones containing hydrocarbon fluids have been identified using perforated drill pipe and packers (Robertson, 2013). WFT data are generally more reliable because of greater sampling capability, more reliable vertical pressure profiles and the ability to acquire measurements at specific depths, whereas DST gauges are usually positioned in the test tool string above the reservoir being tested (Gunter & Moore, 1987). In this study, all DST pressures are plotted at the mid-perforation depth for consistency. Only DST measurements that have been designated as 'final build-ups' are used in the database, as these provide the best representation of true formation pressure.

2.1.3 | Kicks

A kick is defined as any unplanned influx or intrusion of formation fluids into the wellbore, which results in an unexpected gain of fluid into the mud pits, indicative of formation fluid pressure in excess of the weight of the mud column. Quality control methodologies from Lee et al. (2022) were applied to the Taranaki Basin occurrences of wellbore influxes, where shut-in drill pipe pressures (SIDPP) were recorded by removing any erroneous data due to swabbing or wellbore breathing. Kick pressures were calculated using the 'u-tube model', which uses the sum of the estimated downhole pressure exerted by the column of mud in the drill pipe and the shut-in drill pipe pressure (SIDPP) (from a surface gauge):

$$\text{Kick pressure (MPa)} = \\ (\text{Drilling fluid gradient (MPa/m)} \times \text{TVD (m)}) \\ + \text{SIDPP (MPa)}$$

Kicks are especially useful pore pressure measurements as they occur outside of conventional reservoirs with WFT and DST data.

2.1.4 | Mudweight

In the absence of direct pressure measurements, wellbore mudweight can be used as a proxy for pore pressure, using the assumption that mudweights are kept in balance or at slightly greater pressures than the formation pressure (e.g. Webster et al., 2011). Mudweight is usually kept in an overbalance state to prevent influxes in conventional drilling, although it is possible for wells to sometimes be drilled underbalanced, without taking a kick, in very low permeable formations (mudrocks). In this study, fluid pressures calculated from mudweight increases associated with rises in mud gas and fluid influxes due to underbalanced drilling, are used as a proxy for formation pressure.

2.2 | Wireline log data

Pore pressure in fine-grained sediments can be estimated using wireline log data, which exploit the deviation of mudrock properties (e.g. sonic velocities, density and resistivity data) relative to those values typical of a normally compacted sequence at the depth of interest (Webster et al., 2011). Overpressure generated by disequilibrium compaction, as in the Taranaki Basin, is associated with anomalously high sediment porosities (undercompaction) and is thus readily detectable in wireline data (Osborne & Swarbrick, 1997). Deviation in the log data can be used qualitatively to predict porosity anomalies and therefore overpressure maintenance within fine-grained facies.

2.3 | Overpressure determination

A constant hydrostatic gradient of 9.8 MPa/km (8.3 ppg) was used as a reference value for the Taranaki Basin as a basis to calculate from direct pore pressure measurements the degree of overpressure in particular wells in the basin (Robertson et al., 2013). This hydrostatic gradient was calculated from the average value in reservoirs in 21 wells displaying clear aquifer gradients, those wells being widely dispersed across the basin. Applying best-fit straight lines to possible fluid gradients in each well enabled the identification of the most likely type of pore fluid present within the reservoir (i.e. gas, condensate, oil or water) and these were cross-checked against known hydrocarbon accumulations, wireline data and well completion reports (e.g. Robertson et al., 2013).

In all reservoirs that contain a water leg, a value of overpressure representative of the entire reservoir unit was calculated using the shallowest pore pressure measurement interpreted to lie directly on the water gradient. If only hydrocarbons are present, the deepest direct pore pressure measurement interpreted to lie on the hydrocarbon gradient was used to calculate the overpressure. Hydrocarbon buoyancy affects cause overpressure values calculated in the oil or gas leg to be an overestimation of pressure in the water column (Robertson et al., 2013).

2.3.1 | Errors associated with using a constant regional hydrostatic gradient

The use of a constant hydrostatic gradient of 9.8 MPa/km (8.3 ppg) for the entire basin, implies the absence of salinity variation and hence the variation in pore water density across the region, which is an unrealistic assumption and introduces errors in overpressure calculations (Robertson et al., 2013). The gradient across both the Southern Taranaki Inversion Zone and the Western Platform displays a gradient of 10 MPa/km (8.5 ppg), implying that the aquifer is more saline than the areas with a gradient of 9.8 MPa/km. The higher pore water gradient in the two areas noted above probably arises from the incorporation of more fully marine water during sediment accumulation and its subsequent retention within reservoirs than in other areas of the basin. The Eocene to Cretaceous reservoirs in the Central Taranaki Peninsula and in the Manaia Anticline were deposited in coastal plain and marginal marine settings (Higgs et al., 2012; Strogen, 2011), which had fresh to brackish water input. Therefore, reservoirs across the Southern Taranaki Inversion Zone and the Western Platform that appear to be slightly overpressured (ca. 0.7 MPa) are actually hydrostatically pressured.

2.4 | Wireline time-depth conversion

The software named *RokDoc* (v.6.3) was used to calculate depth-to-time conversion for wireline sonic logs from selected wells for plotting in Figures 4, 6 and 8. Check shot data were compiled from well-completion reports.

2.5 | Geopressure province determination

Regions of the basin with similar stratigraphic stacking patterns and structural frameworks were grouped, to form ten provinces. Pore pressure data from wells within these provinces were analysed using multi-well pressure depth plots to identify and test shared trends with depth. The boundaries between these provinces are defined using faults and geobody dimensions, which can act as barriers to flow forming overpressure cells. The most accurate estimation of boundaries was determined using stratigraphic and structural information from published literature and petroleum reports lodged with New Zealand Petroleum and Minerals, a government agency. Not all boundaries are distinct and hence they need to be treated with a degree of uncertainty.

Well-specific pore pressure trends within each province are chiefly dependent on the depth of penetration and the quality of the data collected during drilling. Well density on land in the Taranaki Peninsula and in near-offshore areas is significantly greater than in the deep-water settings of western and north-western parts of the basin, due to the high density of wells associated with known hydrocarbon fields or accumulations. The specific structural styles and stratigraphic stacking patterns within each geopressure province are described in the geopressure province evolution and pore pressure distribution sections below.

3 | RESULTS

3.1 | Geopressure province model

A key outcome of this study is the introduction of a novel geopressure province approach to the interpretation of pore pressure data available for the basin. This approach is considered to have applicability to other basins exhibiting fluid overpressure and displaying polyphase histories or diverse tectonostratigraphic regimes. Ten geopressure provinces have been defined (Figure 1; Table 1). Interpretation of regional seismic lines (Figures 4, 6 and 8) enabled the identification of facies variations between the subareas and structural zones, which are shown to have first-order control on overpressure maintenance and regional fluid flow. See supporting information for a full list of all wells and associated geopressure provinces.

3.2 | Geopressure province structure and pore pressure distribution

3.2.1 | Southern Taranaki Inversion Zone

The Southern Taranaki Inversion Zone (STIZ) (Figure 1) is characterised by a series of inverted Late Cretaceous to Palaeocene grabens and half-grabens, forming a series of

TABLE 1 Summary of geopressure provinces

	Reference well(s)	Key structural features	Key stratigraphic features	Thickness of overpressured mudrocks (m)	Maximum measured overpressure (MPa) & depth (mTVDss)	Top of overpressure (MPa) & depth (mTVDss)
1. Southern Taranaki Inversion Zone	Maui-1	Inverted Late Cretaceous to Palaeocene grabens and half-grabens	Thin Oligocene mudrocks & laterally connected stratigraphy	ca. 75	Normally pressured	
2. Central Taranaki	Te Kiri-2	Very limited inversion	Thick sequences of Miocene mudrock and Pliocene volcanics	ca. 90	Normally pressured	
3. Manaia Anticline	Kupe South-1 & Kapuni Deep-1	Manaia anticlinal ridge	Thick Cretaceous to Late Eocene sandstone beds with numerous mudrock pressure barriers	ca. 250	21.83 5009	6.53 2878
4. Central Taranaki Peninsula	Turangi-3 & Pohokura-3	Inverted Late Cretaceous to Eocene grabens and half-grabens	Stacked Reservoir with varying net-to-gross and connectivity	110–350	22.57 4053	5.36 3169
5. Tarata Thrust Zone	Toetoe-2 & McKee-1	Stacked overthrusts and imbricate wedges	Thrusted blocks entirely confined within Tertiary strata or inter-fingering with basement and Cretaceous-Tertiary strata in mixed stratigraphic order	300–400	13.03 3452	1830 2.55
6. Patea—Whanganui Coast	Kauri-A1	Stacked overthrusts and imbricate wedges	Thrusted blocks comprise allochthonous slivers of basement and Oligocene submarine fans	250–400	22.73 4844	5.42 2422
7. Manganui Platform	Turi-1	Large thrusts and thrust-cored anticlines rooted in the Taranaki Fault	Stacked Reservoir with varying net-to-gross and connectivity	300–700	28.62 3321	9.04 1899
8. Northern Graben		Rapidly subsided grabens	Hydraulically isolated Oligocene—Miocene basin floor fans	>500		
9. Oligocene Sandstones	Tangaroa-1	Structurally undisturbed with regional subsidence and basement h	Hydraulically isolated Tangaroa Formation draped over basement highs	250	14.63 3174	2522 1.88
10. Western Platform	Takapou-1	Structurally undisturbed with regional subsidence and basement highs	Thick sequences of undercompacted Eocene-Miocene mudrock	250–750	Normally pressured	

positive structures (antiforms) along a sequence of north/northeast striking, re-activated reverse faults (e.g. the Maui High; Figure 4a) (Bull et al., 2018; King & Thrasher, 1996; Reilly et al., 2015). In contrast to every other geopressure province, the STIZ does not contain thick sequences of undercompacted Eocene or Oligocene mudrocks, which is the primary stratigraphic interval for the maintenance of excess pressure in the basin (Webster et al., 2011). The geopressure province displays hydrostatic (or near to hydrostatic) pressures, across the entire region and the stratigraphy from the Cretaceous to Pliocene-Pleistocene section (Figure 5a). The mudrock sections in the Maui Field (Figure 4b), albeit thin, act as barriers to vertical flow demonstrated by the differential pressure between stacked reservoirs. The mudrock barriers also act over large distances, shown by the lack of depletion in F-sands in Rahi-1 well (Figure 1), even after significant production (17 years) from the overlying Early Eocene Kaimiro Formation in the Maui Field (20 km away).

3.2.2 | Central Taranaki

The Central Taranaki has been marginal to structure development during the Neogene and is characterised by hydrostatic conditions throughout the stratigraphy (Figure 5b). The Late Miocene inversion of the Southern Taranaki did not extend as far north as Te Kiri-2, but this region received a pulse of sediment from the eroding area to the south, which is expressed as Late Miocene progradation of the shelf-slope margin involving the Mt Messenger and Urenui formations. During the Early Pliocene the Central Taranaki region lay immediately south of the active extension of the Northern Graben and so did not receive the pulse of sediment driving high overpressures to the north. Mount Taranaki, a large andesite volcano formed in the central part of this region around 0.25 Ma, which may be contributing towards the development of underpressures as witness in the Central Taranaki Peninsula province.

3.2.3 | Manaia Anticline

The late mid-Miocene start of shortening in the Southern Taranaki Basin is also expressed in the Manaia Anticline Province as reverse displacement on the Manaia Fault and an associated back-thrust, forming the Manaia anticlinal ridge (Figure 4a). This structure incorporates three separate structural closures forming the Kapuni, Toru and Kupe South fields (Ilg et al., 2012; King & Thrasher, 1996; Voggenreiter, 1993). In the Kupe South area, the Palaeocene Farewell Formation is unconformably overlain by the Oligocene Otaraoa Formation (Martin et al., 1994) and this unconformity cuts down through the stratigraphy towards the Southern Taranaki Basin. Hydrostatic conditions prevail throughout the Neogene section down to the top Oligocene. The nature of the sub-Oligocene unconformity in this region means that the top of the overpressure zone (6.73 MPa, 12.1 MPa/km, 10.3 ppg) across the geopressure province occurs at 2878 mTVDss in the Palaeocene Farewell Formation at Momoho-1, south of the Kupe South Field. Overpressure increases to ca. 9.0 MPa (12.1 MPa/km, 10.3 ppg) with increasing depth in the Kaimiro Formation at Toru-1 (Figure 5c). The overpressure increases again to >20.6 MPa (14 MPa/km, 11.9 ppg) in the Farewell Formation in the Kapuni Field, the highest (75.39 MPa) and deepest (5540 mTVDgl) recorded pore pressure in the basin (Figure 3a) (O'Neill et al., 2018).

Tawa-B1 well (Figure 4a) was drilled into the eastern limb of the Manaia Anticline in the deepest part of the Oligocene foredeep in the footwall of the Taranaki Fault (Strogen, Bland, Nicol, & King, 2014). The Oligocene basin floor fan of the Kauri and Rimu fields are poorly developed in this well, leaving a stratigraphy almost entirely comprised of mudrocks, which become thicker with increasing distance to the west away from the Taranaki Fault. The Otaraoa Formation is >800 mTVD thick in Tawa-B1, meaning it has greater potential for overpressure maintenance, as demonstrated by overpressures in excess of 20 MPa (14 MPa/km, 12 ppg) (Figure 4a). The three kicks taken in Tawa B-1, are associated with a rapid stratigraphic change into predominantly fine-grained facies, which reduces permeability and thus connectivity (Figure 5c).

3.2.4 | Central Taranaki Peninsula

The Central Taranaki Peninsula (Figure 1) contains a series of structures of similar origin to the Manaia Anticline (King et al., 2009; King & Thrasher, 1996), particularly in the northern part of the Peninsula, where numerous small closures occur (Pohokura, Mangahewa, Turangi and Kowhai Fields) upon the same large inversion structure (Figure 6). In contrast to the Manaia Anticline to the south, this geopressure province comprises thick sequences of marine mudrocks and an increase in the occurrence of thin isolated sandstone beds. The top of overpressure (5.36 MPa, 11.4 MPa/km, 9.7 ppg) in the geopressure province occurs in one of these isolated Eocene intra-Turi sandstone beds at 3169 mTVDss. The pressure transition between the Mangahewa Formation and the overlying McKee Formation varies across the region, both in-depth and magnitude (Figure 5d). In Waitui-1 and in the Mangahewa Field, the McKee and Mangahewa formations are in pressure communication, while to the north

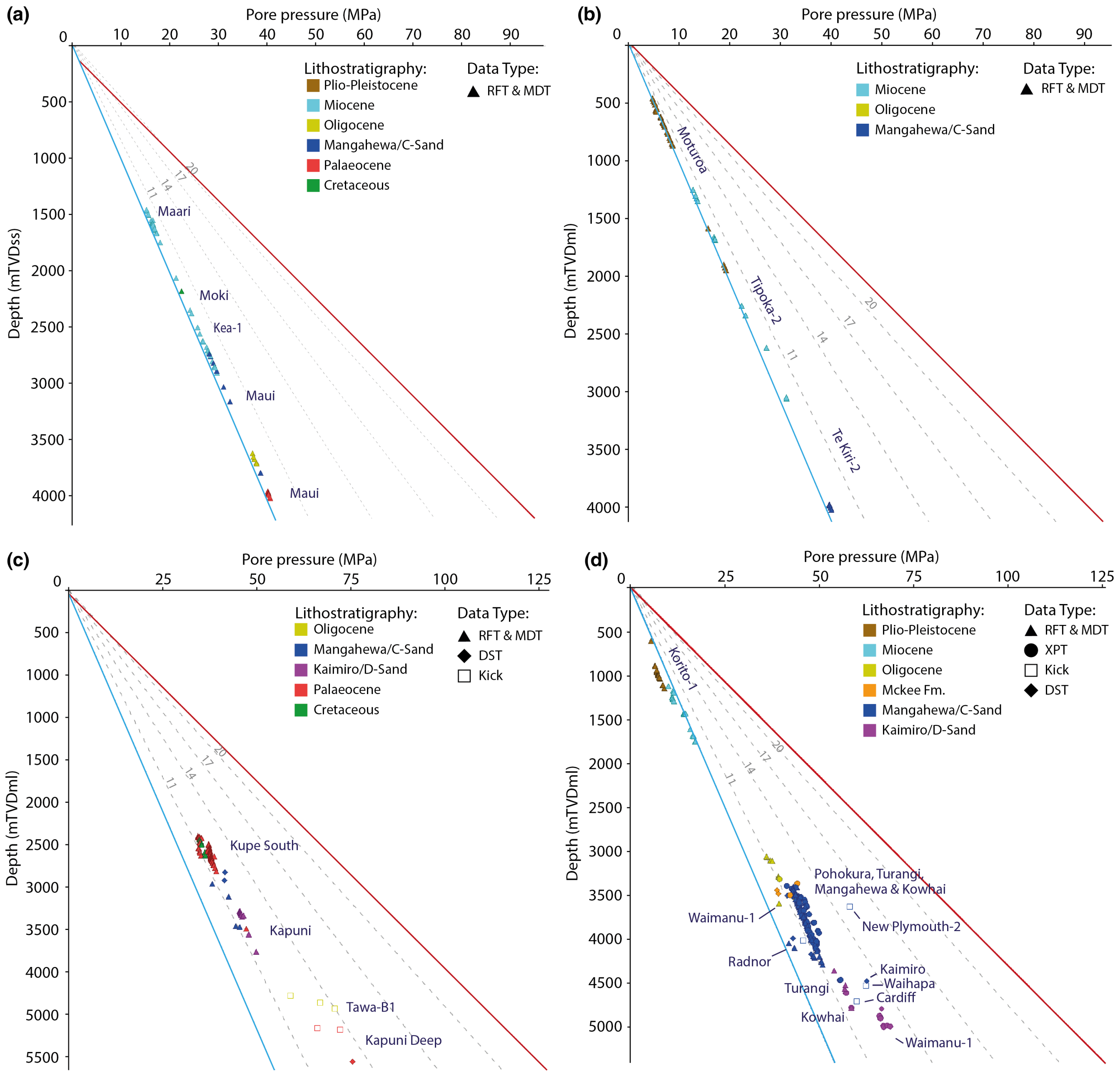

FIGURE 5 Geopressure province multi-well pressure depth plots: (a) Southern Taranaki Inversion Zone; (b) Central Taranaki; (c) Manaia Anticline; and (d) Central Taranaki Peninsula. All plots display only fair and good data (blue line: Hydrostatic pressure; red line: Lithostatic pressure; dashed lines: Pressures gradients in MPa/km).

there is a ca. 1.7 MPa differential in the Pohokura and Turangi fields. The Omata Member (Turi Formation) is present in both this geopressure province and the Manaia Anticline and acts as a vertical pressure barrier within the Early-Mid Eocene, as shown by the 1.38 MPa pressure differential between the Mangahewa and Kaimiro Formations in the Turangi Field (Figures 5c and 6).

The top Eocene is not intercepted until ca. 3900 mTVDss in the northwest of this province at Waimanu-1 and Okoki-1 (Figure 5d), some ca. 600 m deeper than in the eastern part of this province. Waimanu-1 penetrated the Eocene coastal plain in a more distal location, so has a finer grained lithofacies than farther south and displays five separate pressure transitions (Figures 5d and 6). Kowhai-A1R well to the east, influxes and associated increases in mudweight below 4500 mTVD suggest formation pressure in excess of 27 MPa (15.8 MPa/km, 13.4 ppg) above hydrostatic.

The Radnor Field situated in the centre of the peninsula displays three pressure transitions through the Mangahewa Formation, sealed by fine-grained floodplain sequences. Wireline signatures, mudweight and mud log profiles from three outliers (Cardiff, Waihapa & Kaimiro

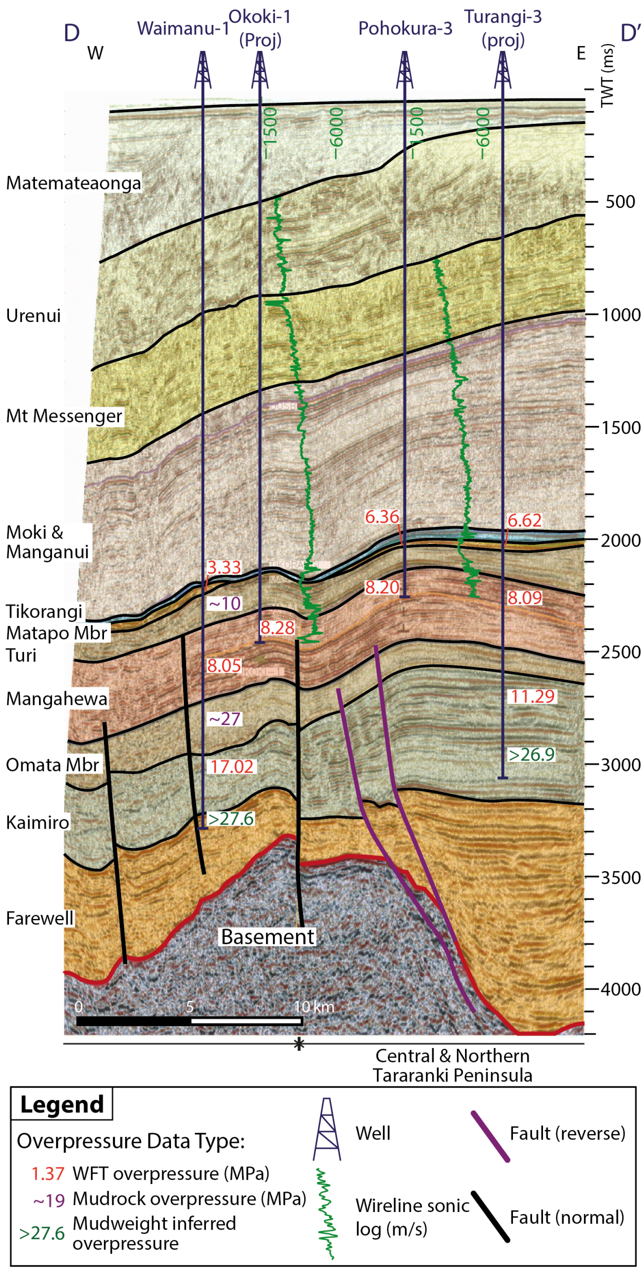

FIGURE 6 Interpreted seismic cross-section through the northern Taranaki Peninsula, displaying both stratigraphic and structural pressure compartmentalisation. (seismic section illustration is modified from Murray, 2000).

Fields) suggest numerous pressure transitions through the Mangahewa Formation due to sealing by interbedded fine-grained horizons. This geopressure province extends underneath the Taranaki Fault as demonstrated by McKee-1 in the following section.

3.2.5 | Tarata Thrust Zone

The Tarata Thrust Zone is located along the basin's eastern margin in the eastern Taranaki Peninsula (Figure 1), with an overall northerly strike, west of and subparallel to, the basin-bounding Taranaki Fault farther east (King & Thrasher, 1996; Stagpoole et al., 2004). The Taranaki Fault comprises multiple laterally and vertically discontinuous and anastomosing slip surfaces that define a series of fault-bound slivers or horse structures (Stagpoole et al., 2004). Thrusted blocks can be entirely confined within Tertiary strata or inter-finger with basement and Cretaceous-Tertiary strata in mixed stratigraphic order (Stagpoole & Nicol, 2008).

The Tarata Thrust Zone comprises thrust faults and duplex structures within mid-Tertiary formations, the thrust faults rooted in the Taranaki Fault Zone to the east. The irregular nature of the hanging wall along the Tarata Thrust Zone and variations in fault zone permeability across it cause vertically stacked overthrust structures to vary between those that are hydraulically isolated and those that are draining in the same well, leading to the trapping of hydrocarbons at multiple levels (Stagpoole et al., 2004). The top of overpressure (2.55 MPa, 11.1 MPa/km, 9.5 ppg) was recorded in a kick at 1830 TVDss (Toetoe-2 well) taken in the Late Eocene McKee Formation of the McKee Field (Figure 7a), which is significantly shallower (ca. 1000 m) than in the Manaia Anticline and the Central Taranaki Peninsula provinces. Thrust sheets in the northern part of the Peninsula have been buried to deeper levels than in the McKee trend in the central-eastern part of the Peninsula, but depth of burial is not a good proxy for overpressure magnitude in this geopressure province, as the Mangahewa Formation is both hydrostatically pressured and significantly overpressured (7.1 MPa) at the same depth in different parts of the field (Figure 7a).

The Ohanga Field has the deepest reservoirs (ca. 3500 mTVDss) in the thrust zone with overpressure values of ca. 7.7 MPa (11.9 MPa/km, 10.1 ppg) in Mangahewa Formation. McKee-1 was drilled to beyond the deepest thrust into a repeated autochthonous section, whereas Beluga-1 was drilled downdip of the McKee Field. Peak pressures (6.2 MPa) recorded in these two wells occur at the same depth. The inherent complexity in this geopressure province is exemplified by the uncertainty around the depth and magnitude of the pressure transition zone between the Mangahewa and McKee formations.

3.2.6 | Patea-Whanganui Coast

The Patea-Whanganui Coast Province is situated towards the south and offshore of the Taranaki Peninsula (Figure 1), differing from the Tarata Thrust Zone in that its overthrust morphologies are directly related to displacements within the Taranaki Fault Zone (Figure 4a). Basement and Cenozoic cover rocks are up-thrown

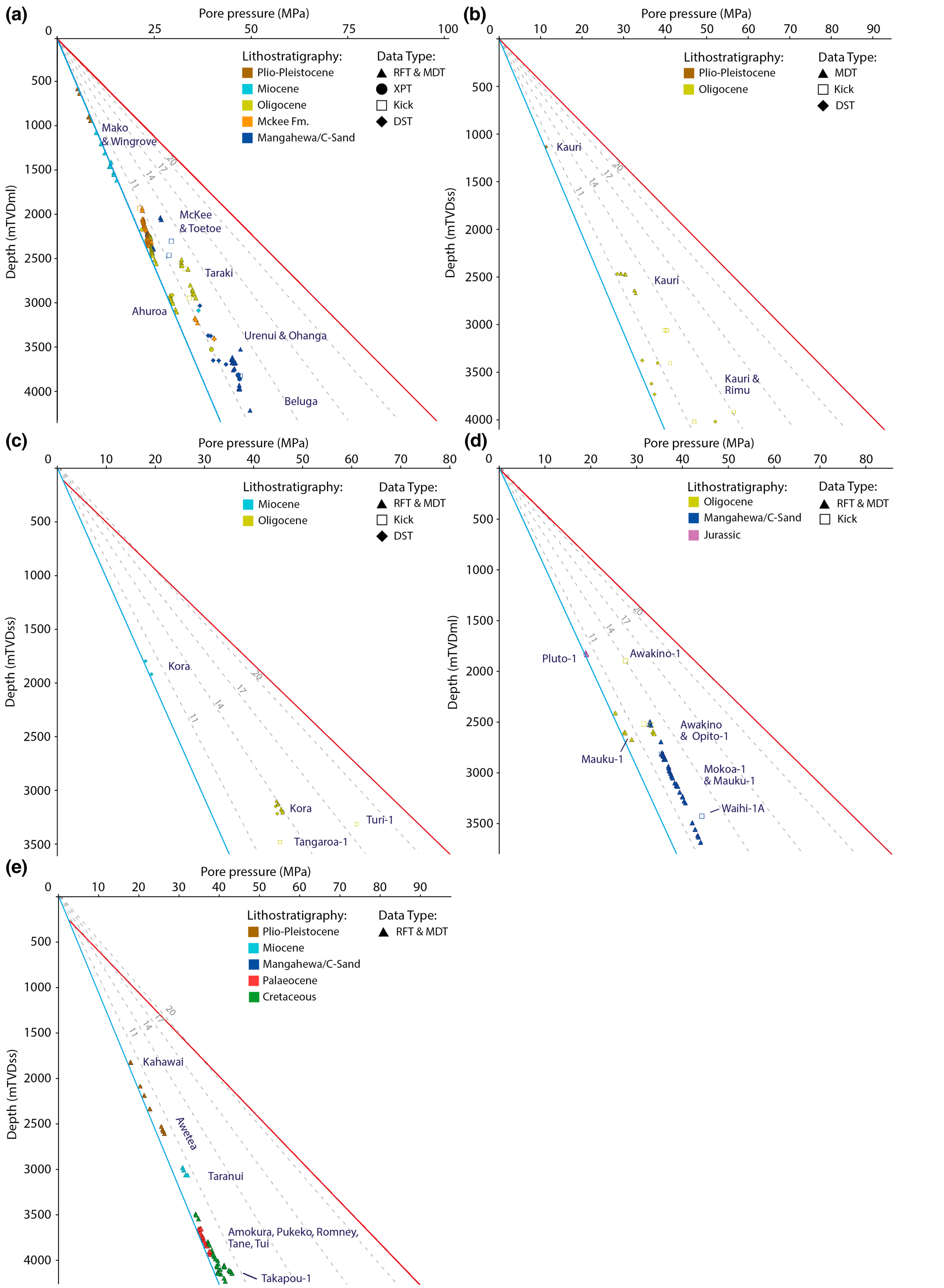

FIGURE 7 Geopressure province multi-well pressure depth plots: (a) Tarata Thrust Zone; (b) Patea-Whanganui Coast; (c) Oligocene Sandstones; (d) Manganui Platform; and (e) Western platform. All plots display only fair and good data (blue line: Hydrostatic pressure; red line: Lithostatic pressure; dashed lines: Pressures gradients in MPa/km).

immediately west of the Taranaki Fault, forming a series of stacked overthrust, imbricate wedges and allochthonous slivers of the basement (Figure 4a), all controlled by west-verging thrust faults (King & Thrasher, 1996). Figure 4a demonstrates how wells (e.g. Kauri-1) can intersect as many as three separate stacked basement thrust sheets. A drill stem test taken in the Tariki Sandstone in Kauri-1 was only slightly overpressured; however, other wells at the same depth are significantly overpressured (>7 MPa) (Figure 7b). As in the Tarata Thrust Zone, the stacked thrust sheets have created traps at multiple levels, acting as independent pressure cells and compartments. Wells in both the Kauri and Rimu fields experienced kicks and formation fluid influxes at multiple levels while drilling proceeded, associated with uncertainty in the depth to, and number of thrust sheets encountered (Figure 7b). Kauri-A4 ST1 experienced two successive kicks of 10.65 and 18.51 MPa (13.2 & 14.5 MPa/km) above hydrostatic, 855 mTVD apart, at the top of two thrust sheets both in the fractured Rimu limestone.

3.2.7 | Manganui Platform

Manganui Platform (Figures 1 and 8) is situated to the north of the Taranaki Peninsula and contains structures (e.g. Awakino Anticline) that lie west of a thrust zone rooted in the Taranaki Fault and can be regarded as structurally similar to the Tarata Thrust Zone but disconnected from it (King & Thrasher, 1996; Stagpoole & Nicol, 2008). Towards the south along this structure, the controlling

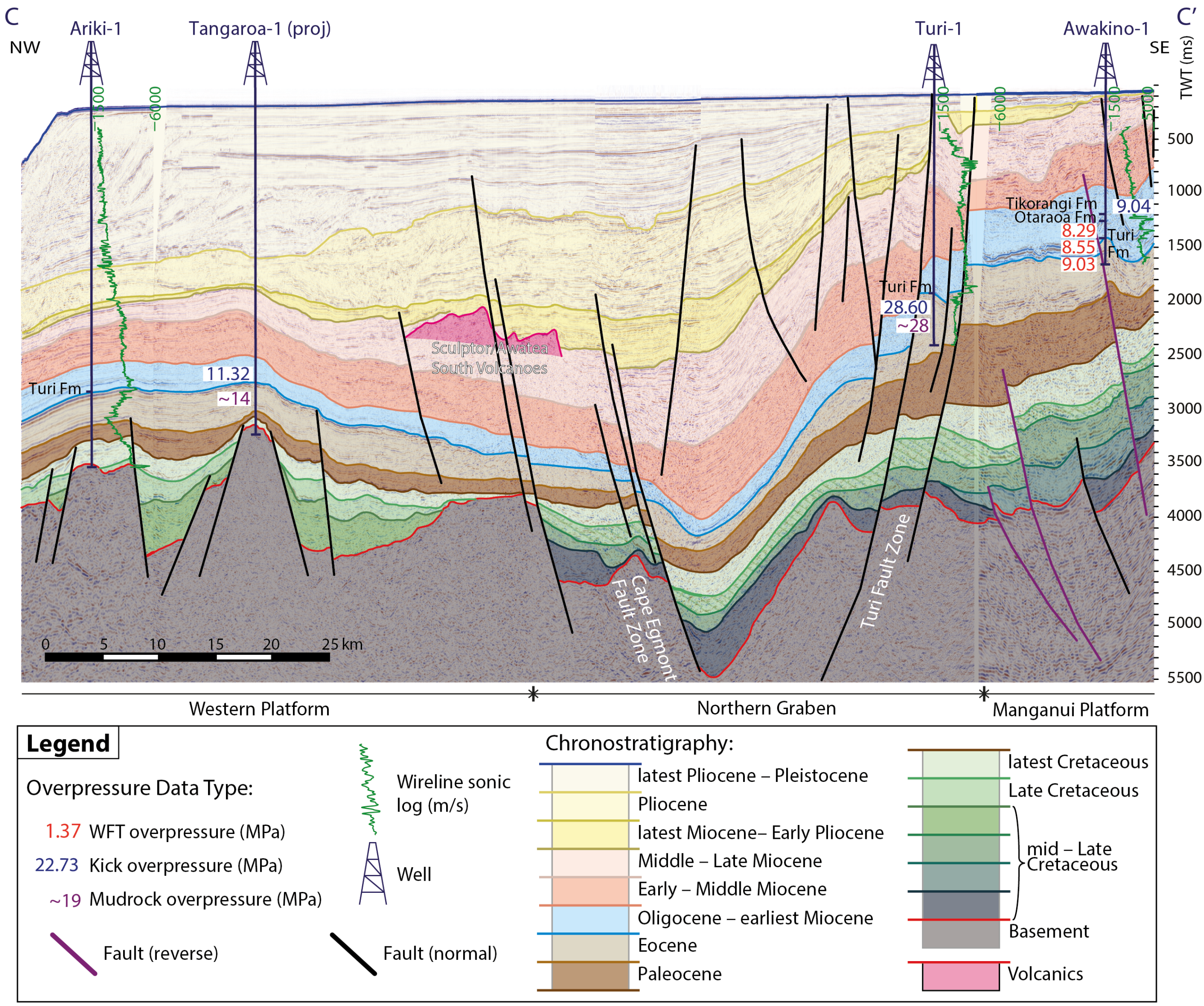

FIGURE 8 Interpreted seismic cross-section through the Manganui Platform, Northern Graben and Northern Taranaki Bight, displaying very high overpressures in isolated sandstone units within the Kapuni Group in the Turi Fault Zone and in the Oligocene Tangaroa sandstone in the North Taranaki Bight (seismic section illustration is modified from Strogen, Bland, Bull, et al., 2014).

displacement on the thrust fault gradually diminishes and the resulting structures in the vicinity of Mokau-1 appear immediately west of the Taranaki Fault (King & Thrasher, 1996). Besides wells drilled into the Awakino Anticline, they have also been drilled into the Mangahewa Formation (e.g. Mauku-1) directly through the tip of a basement overthrust block (e.g. Pluto-1).

The change in vertical motion of the Manganui Platform through the Neogene has led to the development of variable pore pressure regimes. The basin-wide top of significant overpressure (9.04 MPa, 14.5 MPa/km, 12.4 ppg) was recorded from a kick in the fractured Tikorangi Limestone at the crest (1899 mTVDss) of the Awakino Anticline (Figures 7d and 8). Successions of isolated turbidites within the Otaraoa Formation have been intercepted in wells and are better developed north of the peninsula beneath the Manganui Platform. They display a wide variation in the magnitude of overpressures, from 1.71 MPa at Mauku-1 to 9.03 MPa at Awakino-1, linked to the depth of burial and level of geobody connectivity. The Mangahewa Formation in Mokau-1, Mauku-1, Awakino-1 and Waimanu-1 sits on a clear water gradient with the same level of overpressure (8.3 MPa; Figure 7d), which is not too dissimilar to the range in wells within the Central Taranaki Peninsula to the south (ca. 6.9–8.6 MPa; Figure 5d).

3.2.8 | Northern Graben

The Northern Graben (Figures 1 and 8) formed during the latest Miocene to Pliocene and was rapidly filled (up to 700 m/Ma) by sediments of the Mangaa and Giant Foresets formations, contributing over 2000 m of sediment thickness (Hansen & Kamp, 2004; Stagpoole & Funnell, 2001). No deep wells have been drilled in the Northern Graben, but pore pressures approaching fracture pressure could be expected in permeable basin floor fan facies (e.g. Mangaa and Tangaroa Formations), as observed in Turi-1 (Figures 7c, 8 and 9).

3.2.9 | Oligocene sandstones

The Late Eocene and earliest Oligocene Tangaroa Formation (Figures 1, 2 and 8) is comprised of a sequence of fine to medium sandstone beds deposited as a submarine fan within bathyal mudrocks of the Turi Formation (Bloch, 1994; Gresko et al., 1990). The current mapped extent (Strogen, 2011) of the Tangaroa Formation deposits straddle the Northern Graben and Western Platform and are characterised by hydraulically isolated sandstones interbed and enclosed by undercompacted mudrocks. This has led to the maintenance of overpressures of up

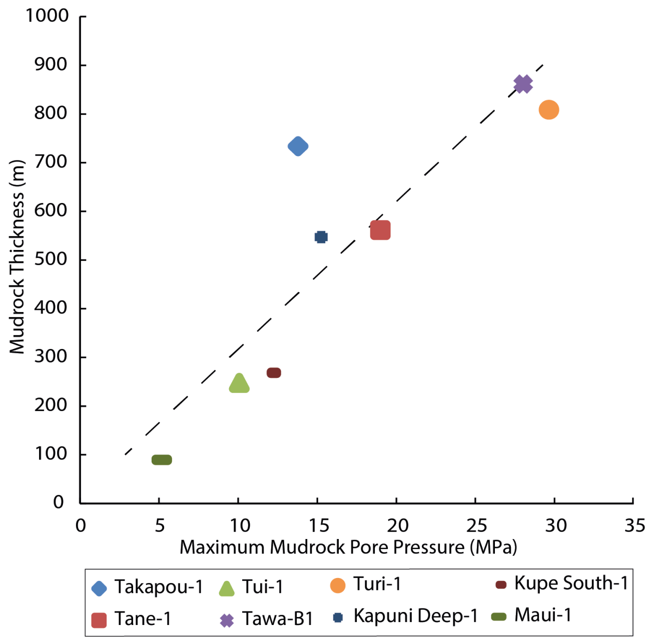

FIGURE 9 Plot of mudrock thickness against maximum mudrock pressure, calculated from wireline sonic logs using the equivalent depth method (well locations in Figure 1).

to 28.6 MPa (18.4 MPa/km, 15.6 ppg), recorded in a kick taken at 3321 mTVDss in sandstone beds in Turi-1 well (Figures 1, 7c, 8 and 9). All the wells that have penetrated the Tangaroa Sandstone have measured overpressure through either direct pressure data (Kora-4 & Tangaroa-1; Figure 7c) or via wireline signatures (Ariki-1; Figure 8). The extent of this geopressure province is based on palaeographic maps showing the coverage of submarine fans as illustrated in Strogen (2011), but these are inherently uncertain, so the reality could differ.

3.2.10 | Western Platform

The Western Platform (Figure 1) has remained relatively tectonically quiescent since the Late Cretaceous except for ongoing slow subsidence (Baur et al., 2014; King & Thrasher, 1996). A shelf-slope wedge prograded onto it during the Miocene to Recent (Kamp et al., 2004) (Figure 4). Almost all of the direct pressure measurements acquired in Western Platform wells (Figure 1) display hydrostatic pressures, with a few exceptions. Takapou-1 shows slight overpressures of 3.94 MPa (10.61 MPa/km, 9 ppg) in the Late Cretaceous section (Figure 7e), while Awatea-1 displays steadily increasing overpressure in three separate isolated fan deposits (0.74–1.88 - 2.98 MPa) all within the Pliocene Mangaa Formation (Webster et al., 2011). A similar pressure depth profile could be expected in the Mangaa Formation sandstones across the Western Platform.

Mudrock pressure estimates within the Oligocene to Eocene section intercepted by Tane-1 and Takapou-1 wells, show overpressures of up to ca. 19 MPa (Figure 4b), suggesting that sandstone beds and mudrock sections are not in equilibrium. Mudrock estimates from the other fully hydrostatic geopressure province, the Southern Taranaki Inversion Zone, are much lower by comparison at ca. 3 MPa (Figure 4a,b). The thickness of the Oligocene to Eocene mudrock section varies from ca. 75 m in the Maui Field at the northern end of the Southern Taranaki Inversion Zone to ca. 700 m at Takapou-1. The deep-water Taranaki Basin has a similar Neogene burial history to that of the Western Platform with loading due to slope progradation, meaning that the Neogene mudrock facies could maintain overpressure but are in equilibrium with permeable formations as demonstrated by the pressure record in Romney-1 (Figure 1).

4 | DISCUSSION

Each of the ten geopressure provinces identified in the Taranaki Basin display its own pore pressure regime, nevertheless linked through a shared stratigraphy and through regional structural and stratigraphic fluid flow pathways (e.g. Figure 10). Facies differences between stratigraphic intervals provide a first-order control on the maintenance and distribution of overpressure, both temporally and spatially across the basin (e.g. Figure 11).

4.1 | Facies variation as a control on overpressure maintenance and distribution

The stratigraphy of the Taranaki Basin is dominated by the occurrence of mud-silt grade facies (ca. 70% by volume; Figure 2), which is the key element for the generation and maintenance of overpressure (Darby, 2002). Overpressure has a tendency to increase basinward from coarse-grained facies at basin margins to mudrocks in deep-water environments (Harrison & Summa, 1991; Javanshir et al., 2015). Hence, a better understanding of the distribution of mudrocks within a basin aids prediction of the likely magnitude of overpressure. Harrison and Summa (1991) used well data from the Gulf of Mexico to define a cut-off of less than 30% sand, after which hydraulic conductivity between stacked permeable sandstone beds is limited enough to maintain excess pressure. This understanding coupled with an appreciation of the connectivity of permeable units within the Taranaki Basin can lead to the identification of fluid flow pathways. In other foreland basin settings such as the South Junggar Depression (Western China) and the Bavarian Molasse Basin, the magnitude of overpressure has been shown to be associated with depositional environments and in particular the thickness of mudrocks in the basin fill (Figure 9) (Drews et al., 2018; Yan et al., 2002).

Pore pressure distribution across a palaeo basin margin (shoreline) is, in part, defined by the development of sequences and their systems tracts. For example, in the Taranaki Basin, transgressive Eocene to Oligocene mudrock beds can act as vertical pressure seals across tens of kilometres perpendicular to the palaeoshoreline (Figure 12a). Facies and formation thicknesses vary significantly across the Taranaki Basin. The variation in net-to-gross of Eocene sandstone beds in the Mangahewa and Kaimiro formations and their associated laterally equivalent mudrocks (Omata Member, Turi Formation) plays a first-order control on the presence and magnitude of preserved overpressure (Table 1). The transect across the Manganui Platform (Figure 8) displays an increase in pore pressure from Awakino-1 to Turi-1 in the Eocene Mangahewa Formation, which is correlated to a significant increase in mudrock volume as the facies grade from a palaeoshoreline in the east to shelfal then bathyal conditions in the northwest (Figure 12a,b) (Higgs et al., 2012). Wireline sonic data plotted against well trajectories in Figure 8, display porosity anomalies below the Tikorangi Limestone, which are an indicator of overpressure preservation (Sayers et al., 2002). The isolated nature of Mangahewa Formation sandstone beds has allowed them to maintain excess pressure, as shown by a good correlation between estimated mudrock pressures and reservoir pressures in Turi-1 (Figure 8).

The transect from the Maui High across the Western Platform to the present shelf-edge break (Figure 4b), displays a gradation within the Eocene section from ca. 90% coarse sandstone facies in the Maui Field to essentially 100% silt-mud grade facies at Tane-1, which is consistent with an east–west change in seismic amplitude from high to low impedance. The estimated mudrock overpressures within the Eocene section range from ca. 3.5 MPa at Maui to ca. 19 MPa at Tane-1 and directly correlate with mudrock volume/thickness (Figures 4b and 9).

The Oligocene Otaraoa Formation and its correlatives not only act as the primary seal to hydrocarbon accumulations in the basin but also maintain overpressure, often in tandem with the Turi Formation. The facies within the Otaraoa Formation do not change significantly, apart from the rare occurrence of thin turbidites fans (Tariki Sandstone Member), but thickness variations (increasing eastward towards the Taranaki Fault) are considerable and correlate with mudrock pressure (Figure 9). The most dramatic thinning of the Otaraoa Formation can be seen in Figure 4a, where the thickness ranges from ca. 800 m at Tawa-B1 in the deepest part of the foredeep, southwestward to ca. 200 m at Toru-1 on the Manaia Anticline, to only ca. 30 m farther west in the Maui Field, which at that time lay near the forebulge position of the foreland basin (King & Thrasher, 1996). This thickness variation with the data available can be directly correlated to increasing mudrock pressure eastward towards the Taranaki Fault. In the Bavarian Molasse Basin, lateral distribution of overpressure correlates with an increase in mudrock volume and deepening and thickening of the wedge-shaped basin from north to south, generating high pore pressures in a similar foredeep position to that of Tawa-B1 (Drews et al., 2018).

4.2 | Compartmentalisation

Faults have been shown to act as barriers to fluid flow in thrusted sections along the Taranaki Fault Zone, in the Turi Fault Zone and between geopressure provinces (Figure 6) but may also operate as conduits to fluid flow (Jolley et al., 2010). Figure 6 shows a section through the Central Taranaki Peninsula Province onto the Manganui Platform Province, which highlights the varying connectivity of reservoirs across the region. Pressure data from four wells that intersect the Eocene Mangahewa Formation indicate hydraulic connectivity between two structures from Okoki-1/Waimanu-1 to Pohokura/Turangi, which does not hold true for other reservoirs. The Matapo Sandstone Member is in pressure communication across the Central Taranaki Peninsula structure but is not present in the syncline or at Okoki-1 and is at lower pressure in Waimanu-1, suggesting that it is a separate geobody. The Early to Mid Eocene Omata Member (Turi Formation) acts as a seal on both sides of the basement high, but the pore pressure values for the Mangahewa Formation are 5.73 MPa higher in Waimanu-1, which suggests that the intervening faults act as barriers to horizontal stratal fluid flow. The low net-to-gross towards the base of these wells, suggests that reverse faults on the eastern side of the structure have entrained fine-grained material from depth, decreasing the permeability of the fault zone. Stratigraphic architecture can also affect hydraulic connectivity through compartmentalisation of parallel geobodies by continuous mudrock layers (Hovadik & Larue, 2010), as shown above in the Oligocene Sandstone Province.

4.3 | Fluid pressure migration pathways

The complex structural architecture of the Eastern Mobile Belt Province provides little opportunity for regional fluid migration. In comparison, the relatively quiescent burial history of the Western Platform Province has allowed for connected stratigraphy to drain excess pressure both laterally and vertically into the generally high net-to-gross Cretaceous to Palaeocene stratigraphy (Strogen, 2011) or permeable faults. Mudrock overpressures estimations in wells (e.g. Tane-1; Figure 4b) on the Western Platform are significantly higher than their associated (underlying) permeable sandstone beds, which suggests that they are not in equilibrium (Figure 4b) and are draining fluid pressure.

Recent rapid loading of the basin by thick Miocene to Pleistocene deposits has led to the formation of fluid escape features. Pockmarks highlight the presence of active or palaeo fluid flow that would aid vertical drainage of pressure (Chenrai & Huuse, 2017). Ilg et al. (2012) have identified the presence of gas chimneys associated with predominantly late-stage (ca. 3.6 Ma) normal faults acting as conduits to flow in southern parts of the Taranaki Basin. These late-stage normal and reverse faults associated with basin inversion could contribute to the dissipation of overpressure vertically, as demonstrated in Brunei (Tingay et al., 2007).

Fluid flow pathways are also present within the stratigraphy of the two geopressure provinces on the eastern basin margin. The lateral transfer of fluid overpressure,

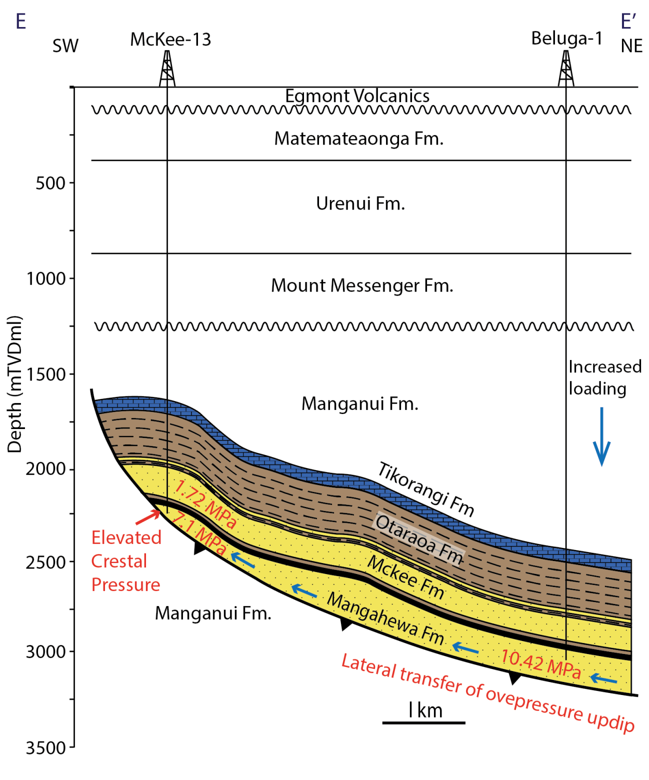

FIGURE 10 Schematic cross-section showing lateral transfer of formation pressure in the Tarata Thrust Zone (modified from Adams et al., 1989).

defined by Yardley and Swarbrick (2000) as the internal redistribution of fluid pressure in a confined and tilted reservoir, can produce elevated crestal pore pressures and occurs via the centroid effect (Bowers, 2001; Dickinson, 1953; Traugott, 1997). This phenomenon can cause challenges in pore pressure prediction, especially in complex environments such as fold and thrust belts (Flemings & Lupa, 2004; Kaeng et al., 2014). The McKee Field in the Tarata Thrust Zone is comprised of several adjoining fault blocks that produce oil, gas and condensate from a steep south-easterly dipping (up to 60°) sandstone reservoir sequence truncated against a deep thrust (Figure 9) (King & Thrasher, 1996). If we assume that the Mangahewa Formation is confined and in lateral continuity, the excess pressure maintained downdip (Beluga-1 well; Figure 9) could be migrating up dip via the centroid effect. The dipping nature of many of the deep-rooted thrusted reservoir sequences across the Tarata Thrust Zone and Patea-Whanganui Coast (e.g. Figure 4a) implies that lateral transfer may be occurring across the eastern basin margin.

4.4 | Fluid pressure transitions

Pressure transition zones, defined by Swarbrick and Osborne (1996), occur where the rate of increase in pressure with depth exceeds the increase attributable to the density of the formation fluids. Disequilibrium compaction induced transition zones are characterised by relatively abrupt deviations from the hydrostatic gradient, below which almost all pore fluids are retained (Swarbrick & Osborne, 1996), as highlighted in numerous rapidly subsiding Tertiary Basins (Nile Delta, Niger Delta, Gulf of Mexico & Taranaki Basin) (Badri et al., 2000; Bilotti & Shaw, 2005; Dickinson, 1953; Webster et al., 2011).

Rapid increases in pore pressure have been documented in the mudweight profiles of wells penetrating >5000 mTVDgl on the Taranaki Peninsula and wells >ca. 3500 mTVDss on the north-western Manganui Platform (Figure 11). Mudweight can be used as a proxy for formation pressure, especially when increases are due to wellbore kicks or dynamic fluid influx, as was the case with all of these wells. One recent deep well, Kowhai-A1R (Figure 11), required a kill mudweight equal to an overpressure of ca. 27 MPa (15.8 MPa/km, 13.4 ppg) to address a fluid influx. The well penetrated farewell formation at the distal part of the Palaeocene coastal plain sequence, which is exemplified by a substantial increase in mudrock volume (mud log and in wireline signatures), and thus potential to maintain overpressures. The mud log implies that the drilling

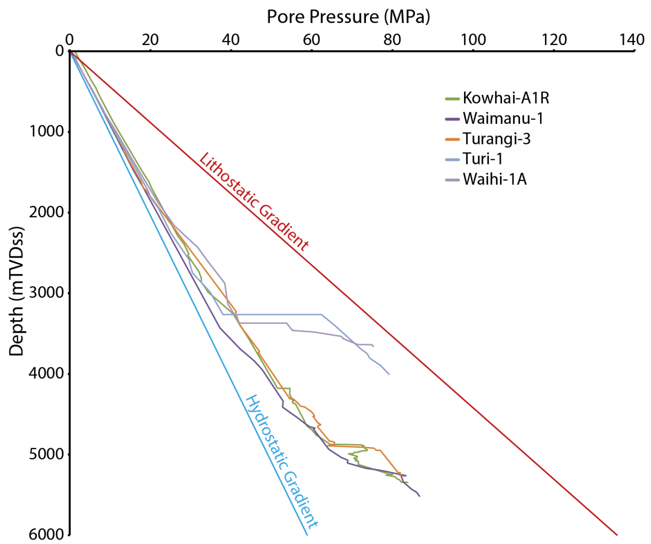

FIGURE 11 Mudweight depth profiles for specific wells in the Central Taranaki Peninsula area and on the Manganui Platform.

break occurred in soft, friable, very fine-grained and weakly calcareous sandstone, which is overlain by a hard calcareous concretionary layer. This suggests the occurrence of a vertical pressure barrier of diagenetic origin, as discussed in a case study from Kapuni Deep-1 on the Manaia Anticline (O'Neill et al., 2018).

Figure 12a displays the mapped extent of shoreline facies (reservoir sandstone) for the major reservoir intervals within the Taranaki Basin and associated wells that were drilled close to these boundaries. Kowhai-A1R was drilled close to the northwest extent of shoreline facies of the Early Eocene Kaimiro Formation, terminating in a thick sequence of undercompacted mudrocks, which are suggested to be contributing to the preservation of overpressure at depth. In all the wells in Figure 12b,c, mudrock volume increases dramatically towards the well termination depth, associated with an increase in the formation pressure of adjacent sandstone beds. The rapid decrease in net sand leads to a reduction in hydraulic connectivity, thereby limiting the permeability to a point where the majority of the excess pressure is maintained, producing relatively abrupt pressure transitions indicative of disequilibrium compaction (Swarbrick & Osborne, 1996). Porosity anomalies and associated significant deviation of wireline sonic data below the Tikorangi Limestone support this hypothesis (Sayers et al., 2002) (Figure 8).

4.5 | Overpressure & underpressure mechanisms

Overpressure maintenance through disequilibrium compaction has been shown to be the driving mechanism in overpressure maintenance across the Taranaki Basin

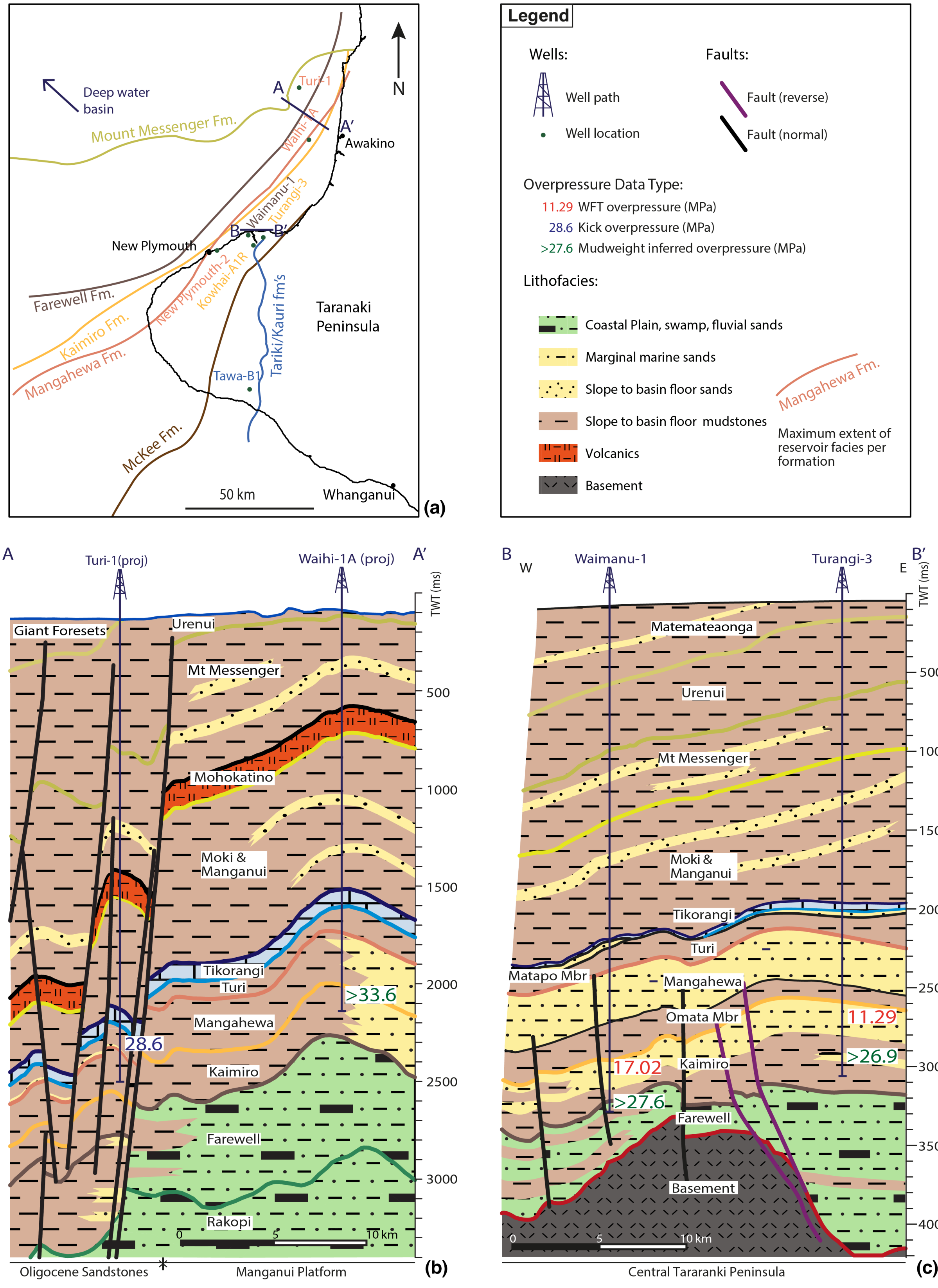

FIGURE 12 (a) The outer, north-western extents of sandstone distribution in the labelled main reservoir formations in the Taranaki Basin. The font colour of well name correlates with the colour of the formation line (modified from Strogen, 2011). (b) Interpreted seismic cross-section through Waihi-1A & Turi-1 wells, including facies distribution. (c) Interpreted seismic cross-section through Waimanu-1 & Turangi-3, including facies distribution (seismic section illustrations are modified from Strogen, Bland, Bull, et al., 2014).

(Webster et al., 2011), and this work has highlighted no further compelling evidence to suggest further secondary mechanisms. Pressure predictions from wireline logs using the equivalent depth method (Hottmann & Johnson, 1965) are very close to measured pore pressure (demonstrated in Turi-1; Figure 8), showing that compaction-related mechanisms can account alone for the overpressures. Uplift in the eastern Taranaki Basin may have led to the preservation of anomalously high overpressures at shallow depths, but uplift in the Southern Inversion zone has resulted in reservoir drainage. Also, rapidly uplifted reservoirs surrounding Mount Taranaki are underpressured, which has been demonstrated in the laboratory environment (Neuzil & Pollock, 1983) and basins worldwide (Birchall et al., 2019).

Hydrocarbon generation, especially kerogen to gas maturation, has been considered the principal overpressure generating mechanism in certain basins (Amazon Fan, Kutai Basin & Malay Basin), which are associated with significant transition zones of up to 15 MPa/km (Cobbold et al., 2004; Ramdhan & Goulty, 2010; Tingay et al., 2013). The presence of significant gas cuts in deep well influx hints at the possibility of gas expansion and kerogen cracking as a further overpressure generating mechanism, though this is difficult to test as coaly source rocks do not lend themselves to wireline log response methodologies as with mudrocks (Swarbrick et al., 2002).

The Miocene to Recent section in the Taranaki Basin, for the most part, is normally pressured across the basin, but wells drilled in the foothills of Mt. Taranaki have highlighted the occurrence of underpressure in the Plio-Pleistocene section (Figure 3a,b), even with a sea level correction applied. The geological mechanisms for the occurrence of underpressure were outlined by Swarbrick and Osborne (1998) as (a) differential recharge/discharge of reservoirs, (b) deflationary pressures during elastic rebound on uplift, (c) thermal contraction of fluid and (d) location of a well at a site where the water table is substantially below Earth's surface. The Central Taranaki Peninsula and the area to the east have experienced Quaternary (<2 Ma) uplift of ca. 2 km due to the uplift of the North Island (Kamp et al., 2004) and have large variations in water table elevation due to seasonal discharge variations.

4.6 | Disadvantages of the geopressure province model

The lack of wellbore penetrations in certain provinces can cause calibration difficulties over wide areas, resulting in a greater reliance on the use of palaeogeography and structural reconstructions in defining the boundaries between provinces. The Northern Graben for example has no deep >2000 m wellbore penetration, which makes calibration very difficult, meaning that pore pressure estimation is reliant upon sedimentation and burial rate approximations and seismic velocities. The actual depositional extent of Oligocene-Pleistocene deep-water fans (permeable formations), like the Mangaa and Tangaroa Formations, is highly uncertain, which may have consequences upon basin plumbing and the definition of province boundaries. A related issue is the potential disparity between reservoir formation pressures and mudrock pressure estimations, as they are often not in equilibrium. This study has had a greater focus on the more permeable formations, which have been shown to be drained with respect to the surrounding mudrocks.

4.7 | Implications for sedimentary basins

Measured pore fluid pressure data are routinely collected during drilling operations but are rarely discussed in the context of a basin's tectonostratigraphic development or regional variations in fluid pressure. This study highlights the great value of pore fluid pressure data and their implications for structural geology, facies analysis, geohazards, gas storage, drilling operations and regional subsurface fluid flow. Knowledge of pore pressure distribution within a basin can also be used in prospecting activity for suitable reservoirs for gas storage (e.g. Carbon Dioxide, Methane or Hydrogen) (Dewers et al., 2018) and in exploration for geothermal fluid reservoirs.

Direct pore pressure measurements are typically restricted to permeable formations encountered in drilling, which alone cannot define the distribution of pore pressure across a sedimentary basin, as overpressures are maintained in mudrocks adjacent to permeable formations, and the two are often not in equilibrium (Zhang, 2011). The application of mudrock pressure estimation methodologies allows for the definition of magnitude and variation in maintained overpressures across a basin and the identification of potential fluid flow pathways. Overpressure distributions within permeable facies are strongly influenced by long-range pressure interactions caused by horizontal and vertical flows (Hantschel & Kauerauf, 2009). Mudrock lithofacies, thickness and distribution are shown to exert a first-order control on pore pressure distributions. The connected nature of deep permeable stratigraphic units and complex interplays with associated mudrocks in the Taranaki Basin, provide an excellent analogue for tectonostratigraphically diverse basins, which can be investigated using wireline log and compaction data.

The maintenance of excess pore fluid pressures is not solely defined by stratigraphic or structural controls but often by a combination of the two. The pore pressure regime in geopressure province on the Eastern Mobile Belt is defined by laterally sealing faults, which hydraulically isolate adjacent reservoirs of the same age. The Tarata Thrust Zone also provides an excellent example of inherent variations in pressure both laterally and vertically, which can be used to express the level of uncertainty and to better calibrate pore pressure predictions in fold and thrust belts (e.g. Couzens-Schultz & Azbel, 2014; Roure et al., 2010).

Pore fluid pressure has also been implicated as a driver of seismic activity and fault propagation (Leclère et al., 2015) in both extensional (Morley & Naghadeh, 2017) and compressional settings (Wallace et al., 2017) as it plays a primary mechanical role during faulting by reducing effective normal stress and the required shear stress for sliding. Recent modelling has demonstrated that pore fluid pressure magnitude is directly related to nucleation length and duration of the nucleation phase during faulting (Snell et al., 2019).

5 | CONCLUSIONS

1. The interpretation of pore pressure data at basin scale within the Taranaki Basin has been shown to be best explained by consideration of the basin as ten geopressure provinces, each having its own distinctive pore pressure profiles defined by their stratigraphic architecture and structural development.
2. Facies variations across stratigraphic intervals provide a first-order control on hydraulic conductivity within interbedded sandstone and mudrock successions, which has in turn defined the level of overpressure maintenance and distribution across the Taranaki Basin.
3. Cretaceous to Early Miocene formations are both normally pressured (near or at hydrostatic) and significantly overpressured (up to 28 MPa, 3321 mTVDss) at the same depth in separate parts of the basin.
4. Faults have been shown to act as barriers to lateral and vertical fluid flow in the Tarata Thrust Zone, in the Patea-Whanganui Coast area and in the Turi Fault Zone, but they can also define barriers between geopressure provinces.
5. Repeated stratigraphic slices due to thrust faulting along the eastern basin margin place major uncertainty on the prediction of the stratigraphic stacking pattern and on associated facies architecture away from wells.
6. Deep pressure transitions in the basin have been shown to occur across sealing horizons caused by diagenetic, structural and stratigraphic mechanisms and generated by an increase in mudrock volume (reduced permeability) or gas generation.
7. Pore pressure distributions and significant increases with depth across the palaeoshoreline are defined by the development of sequences, their systems tracts and associated lithofacies.

ACKNOWLEDGEMENTS

The work contained in this paper was conducted during a PhD study undertaken as part of the Natural Environment Research Council Centre for Doctoral Training (CDT) in Oil & Gas [grant number NEM00578X/1] and is fully funded by NERC whose support is gratefully acknowledged. PJJK acknowledges MBIE research funding CONT-42907-EMTR-UOW, and SRON acknowledges support from the University of Waikato Postdoctoral Research Fellowship. The authors acknowledge IKON Science for the use of RokDoc software. The authors acknowledge Robert Crookburn (Shell Taranaki Ltd.) for his assistance during the formative stages of this research. The manuscript was improved after discussions with Andy Aplin, Richard Swarbrick, and Mark Allen. The authors acknowledge Mark Tingay, Mads Huuse, Rob Funnell, Connor O'Sullivan and one anonymous reviewer, for their thorough and constructive reviews.

CONFLICT OF INTEREST

The authors have no conflict of interest.

DATA AVAILABILITY STATEMENT

The data that support the findings of this study are available in the supplementary material.

ORCID

Sean R. O'Neill https://orcid.org/0000-0002-0497-6989
Stuart J. Jones https://orcid.org/0000-0001-5897-2695
Peter J. J. Kamp https://orcid.org/0000-0002-2563-884X

REFERENCES

Adams, M., Kelly, C., & Khasi, K. (1989). *Mckee-8 well completion report. PML38086: Ministry of Economic Development Unpublished Petroleum Report 1458*.

Badri, M., Sayers, C., Awad, R., & Graziano, A. (2000). A feasibility study for pore-pressure prediction using seismic velocities in the offshore Nile Delta, Egypt. *The Leading Edge*, *19*(10), 1103–1108. https://doi.org/10.1190/1.1438487

Baur, J., Sutherland, R., & Stern, T. (2014). Anomalous passive subsidence of deep-water sedimentary basins: A prearc basin example, southern New Caledonia trough and Taranaki Basin, New Zealand. *Basin Research*, *26*(2), 242–268. https://doi.org/10.1111/bre.12030

Bilotti, F., & Shaw, J. H. (2005). Deep-water Niger Delta fold and thrust belt modeled as a critical-taper wedge: The influence of elevated basal fluid pressure on structural styles. *AAPG Bulletin*, *89*(11), 1475–1491. https://doi.org/10.1306/06130505002

Birchall, T., Swarbrick, R., & Senger, K. (2019). Naturally occurring underpressure—A global perspective. *2019 AAPG Annual Convention and Exhibition*.

Bloch, S. (1994). Case histories—Offshore Mid-Norway/Taranaki Basin, New Zealand/San Emigdio Area, California. In M. D. Wilson (Ed.), *Reservoir quality assessment and prediction in clastic rocks*. SEPM Society for Sedimentary Geology. https://doi.org/10.2110/scn.94.30.0357

Borge, H. (2002). Modelling generation and dissipation of overpressure in sedimentary basins: An example from the Halten Terrace, offshore Norway. *Marine and Petroleum Geology*, *19*, 377–388. https://doi.org/10.1016/S0264-8172(02)00023-5

Bowers, G. L. (2001). Determining an appropriate pore-pressure estimation strategy. *Offshore Technology Conference*, 1–14. https://doi.org/10.4043/13042-MS

Bull, S., Nicol, A., Strogen, D., Kroeger, K. F., & Seebeck, H. S. (2018). Tectonic controls on Miocene sedimentation in the southern Taranaki Basin and implications for New Zealand plate boundary deformation. *Basin Research*, *31*, 253–273. https://doi.org/10.1111/bre.12319

Burgreen-Chan, B., Meisling, K. E., & Graham, S. (2016). Basin and petroleum system modelling of the East Coast Basin, New Zealand: A test of overpressure scenarios in a convergent margin. *Basin Research*, *28*(4), 536–567. https://doi.org/10.1111/bre.12121

Chenrai, P., & Huuse, M. (2017). Pockmark formation by porewater expulsion during rapid progradation in the offshore Taranaki Basin, New Zealand. *Marine and Petroleum Geology*, *82*, 399–413. https://doi.org/10.1016/j.marpetgeo.2017.02.017

Cobbold, P. R., Mourgues, R., & Boyd, K. (2004). Mechanism of thin-skinned detachment in the Amazon Fan: Assessing the importance of fluid overpressure and hydrocarbon generation. *Marine and Petroleum Geology*, *21*(8), 1013–1025. https://doi.org/10.1016/j.marpetgeo.2004.05.003

Couzens-Schultz, B. A., & Azbel, K. (2014). Predicting pore pressure in active fold e thrust systems: An empirical model for the deepwater Sabah foldbelt. *Journal of Structural Geology*, *69*, 465–480. https://doi.org/10.1016/j.jsg.2014.07.013

Crowhurst, P. V., Green, P. F., & Kamp, P. J. J. (2002). Appraisal of (U-Th)/He apatite thermochronology as a thermal history tool for hydrocarbon exploration: An example from the Taranaki Basin, New Zealand. *AAPG Bulletin*, *86*(10), 1801–1819. https://doi.org/10.1306/61EEDD82-173E-11D7-8645000102C1865D

Darby, D. (2002). Seal properties, overpressure and stress in the Taranaki and East Coast Basins, New Zealand. *2002 New Zealand Petroleum Conference Proceedings*, *2*(February), 1–10.

Darby, D., Haszeldine, R. S., & Couples, G. D. (1996). Pressure cells and pressure seals in the UK Central Graben. *Marine and Petroleum Geology*, *13*(8), 865–878. https://doi.org/10.1016/S0264-8172(96)00023-2

de Bock, J. F., Palmer, J. A., & Lock, R. G. (1990). Tariki Sandstone—Early Oligocene hydrocarbon reservoir, eastern Taranaki, New Zealand. *New Zealand Petroleum Conference*, 214–224.

Dewers, T., Eichhubl, P., Ganis, B., Gomez, S., Heath, J., Jammoul, M., Kobos, P., Liu, R., Major, J., Matteo, E., Newell, P., Rinehart, A., Sobolik, S., Stormont, J., Reda Taha, M., Wheeler, M., & White, D. (2018). Heterogeneity, pore pressure, and injectate chemistry: Control measures for geologic carbon storage. *International Journal of Greenhouse Gas Control*, *68*, 203–215. https://doi.org/10.1016/j.ijggc.2017.11.014

Dickinson, G. (1953). Geological aspects of abnormal reservoir pressures in Gulf Coast Louisiana. *AAPG Bulletin*, *37*(2), 410–432. https://doi.org/10.1306/5CEADC6B-16BB-11D7-8645000102C1865D

Drews, M. C., Bauer, W., Caracciolo, L., & Stollhofen, H. (2018). Disequilibrium compaction overpressure in shales of the Bavarian foreland Molasse Basin: Results and geographical distribution from velocity-based analyses. *Marine and Petroleum Geology*, *92*, 37–50. https://doi.org/10.1016/j.marpetgeo.2018.02.017

Flemings, P. B., & Lupa, J. A. (2004). Pressure prediction in the Bullwinkle Basin through petrophysics and flow modeling (Green Canyon 65, Gulf of Mexico). *Marine and Petroleum Geology*, *21*(10), 1311–1322. https://doi.org/10.1016/j.marpetgeo.2004.09.005

Giba, M., Nicol, A., & Walsh, J. J. (2010). Evolution of faulting and volcanism in a back-arc basin and its implications for subduction processes. *Tectonics*, *29*(4).

Gresko, M., Jordan, D. W., & Thompson, P. R. (1990). A Sequence Stratigraphic Study of the Tangaroa Sandstone, Taranaki Basin, New Zealand. *AAPG Annual Convention Conference Preceedings*.

Gunter, J. M., & Moore, C. V. (1987). Improved use of wireline testers for reservoir evaluation. *Journal of Petroleum Technology*, *39*(6), 635–644. https://doi.org/10.2118/16481-PA

Hansen, R. J., & Kamp, P. J. J. (2004). Late Miocene to early Pliocene stratigraphic record in northern Taranaki Basin: Condensed sedimentation ahead of northern Graben extension and progradation of the modern continental margin. *New Zealand Journal of Geology and Geophysics*, *47*(4), 645–662. https://doi.org/10.1080/00288306.2004.9515081

Hantschel, T., & Kauerauf, A. I. (2009). Fundamentals of basin and petroleum systems modeling. In *Fundamentals of basin and petroleum systems modeling*. Springer-Verlag. https://doi.org/10.1007/978-3-540-72318-9

Harrison, W. J., & Summa, L. L. (1991). Paleohydrology of the Gulf of Mexico Basin. *American Journal of Science*, *291*(2), 109–176. https://doi.org/10.2475/ajs.291.2.109

He, S., & Middleton, M. (2002). Pressure seal and deep overpressure modelling in the Barrow sub-basin, north west shelf, Australia. *Proceedings of The Sedimentary Basins of Western Australia*, *3*, 531–549.

Higgs, K. E., Strogen, D. P., Griffin, A., Ilg, B. R., & Arnot, M. J. (2012). *Reservoirs of the Taranaki Basin, New Zealand*. GNS Science Data Series No. 2012/13a.

Holt, W. E., & Stern, T. A. (1994). Subduction, platform subsidence, and foreland thrust loading: The late Tertiary development of Taranaki Basin, New Zealand. *Tectonics*, *13*(5), 1068–1092. https://doi.org/10.1029/94TC00454

Hood, S. D., Nelson, C. S., & Kamp, P. J. J. (2003). Lithostratigraphy and depositional episodes of the Oligocene carbonate-rich Tikorangi formation, Taranaki Basin, New Zealand. *New Zealand Journal of Geology and Geophysics*, *46*(3), 363–386. https://doi.org/10.1080/00288306.2003.9515015

Hottmann, C. E., & Johnson, R. K. (1965). Estimation of formation pressures from log-derived shale properties. *Journal of Petroleum Technology*, *17*(6), 717–722. https://doi.org/10.2118/1110-PA

Hovadik, J. M., & Larue, D. K. (2010). Stratigraphic and structural connectivity. *Geological Society Special Publications*, *347*(1), 219–242. https://doi.org/10.1144/SP347.13

Ilg, B. R., Hemmings-Sykes, S., Nicol, A., Baur, J., Fohrmann, M., Funnell, R., & Milner, M. (2012). Normal faults and gas migration in an active plate boundary, southern Taranaki Basin, offshore New Zealand. *AAPG Bulletin*, *96*(9), 1733–1756. https://doi.org/10.1306/02011211088

Iliffe, J. E., Robertson, A. G., Ward, G. H. F., Wynn, C., Pead, S. D. M., & Cameron, N. (1999). The importance of fluid pressures and migration to the hydrocarbon prospectivity of the Faeroe-Shetland White Zone. *Petroleum Geology of Northwest Europe; Proceedings of the 5th Conference*, *5*, 600–611. https://doi.org/10.1144/0050601

Javanshir, R. J., Riley, G. W., Duppenbecker, S. J., & Abdullayev, N. (2015). Validation of lateral fluid flow in an overpressured sand-shale sequence during development of Azeri-Chirag-Gunashli oil field and Shah Deniz gas field: South Caspian Basin, Azerbaijan. *Marine and Petroleum Geology*, *59*, 593–610. https://doi.org/10.1016/j.marpetgeo.2014.07.019

Jolley, S. J., Fisher, Q. J., & Ainsworth, R. B. (2010). Reservoir compartmentalization: An introduction. *Geological Society, London, Special Publications*, *347*(1), 1–8. https://doi.org/10.1144/SP347.1

Kaeng, G. C., Sausan, S., & Satria, A. (2014). Geopressure centroid as pore pressure prediction challenge in Deepwater South East Asia. *International Petroleum Technology Conference*, *11*. https://doi.org/10.2523/IPTC-18239-MS

Kamp, P. J. J., & Green, P. F. (1990). Thermal and tectonic history of selected Taranaki Basin (New Zealand) wells assessed by apatite fission track analysis. *American Association of Petroleum Geologists Bulletin*, *74*(9), 1401–1419. https://doi.org/10.1306/0C9B24E3-1710-11D7-8645000102C1865D

Kamp, P. J. J., Tripathi, A. R. P., & Nelson, C. S. (2014). Paleogeography of late Eocene to earliest Miocene Te Kuiti group, central-western North Island, New Zealand. *New Zealand Journal of Geology and Geophysics*, *57*(2), 128–148. https://doi.org/10.1080/00288306.2014.904384

Kamp, P. J. J., Vonk, A. J., Bland, K. J., Hansen, R. J., Hendy, A. J. W., McIntyre, A. P., Ngatai, M., Cartwright, S. J., Hayton, S., & Nelson, C. S. (2004). Neogene stratigraphic architecture and tectonic evolution of wanganui, king country, and eastern taranaki basins, New Zealand. *New Zealand Journal of Geology and Geophysics*, *47*(4), 625–644. https://doi.org/10.1080/00288306.2004.9515080

King, P. R., Bland, K. J., & Lever, L. (2009). *Opportunities for underground geological storage of CO_2 in New Zealand—Report CCS-08/5—Onshore Taranaki Basin overview*. (Issue December).

King, P. R., & Thrasher, G. P. (1996). *Cretaceous-Cenozoic Geology and Petroleum Systems of the Taranaki Basin, New Zealand*. Institute of Geological and Nuclear Sciences, Monograph 13, Ministry of Economic Development Petroleum Report 3224.

Leap Energy. (2014). *Leap Energy's New Zealand ArcGIS Geodatabase*.

Leclère, H., Cappa, F., Faulkner, D., Fabbri, O., Armitage, P., & Blake, O. (2015). Development and maintenance of fluid overpressures in crustal fault zones by elastic compaction and implications for earthquake swarms. *Journal of Geophysical Research: Solid Earth*, *120*, 4450–4473. https://doi.org/10.1002/2014JB011759

Lee, J., Swarbrick, R., & O'Connor, S. (2022). Kicks and their significance in pore pressure prediction. *Petroleum Geoscience*, *28*(2), petgeo2021-061. https://doi.org/10.1144/petgeo2021-061

Martin, K. R., Baker, J. C., Hamilton, P. J., & Thrasher, G. P. (1994). Diagenesis and reservoir quality of Palaeocene sandstones in the Kupe south field, Taranaki Basin, New Zealand. *AAPG Bulletin*, *78*(4), 624–643.

Masalimova, L. U., Lowe, D. R., Sharman, G. R., King, P. R., & Arnot, M. J. (2016). Outcrop characterization of a submarine channel-lobe complex: The lower mount messenger formation, Taranaki Basin, New Zealand. *Marine and Petroleum Geology*, *71*, 360–390. https://doi.org/10.1016/j.marpetgeo.2016.01.004

Mattos, N. H., Alves, T. M., & Scully, A. (2018). Structural and depositional controls on Plio-Pleistocene submarine channel geometry (Taranaki Basin, New Zealand). *Basin Research*, *v31*(1), 136–154. https://doi.org/10.1111/bre.12312

Mitchell, J. S., Mackay, K. A., Neil, H. L., Mackay, E. J., Pallentin, A., & Notman, P. (2012). *Undersea New Zealand, 1:5,000,000*. NIWA Chart, Miscellaneous Series No. 92.

Morley, C. K., & Naghadeh, D. H. (2017). Tectonic compaction shortening in toe region of isolated listric normal fault, North Taranaki Basin, New Zealand. *Basin Research*, *v30*, 424–436. https://doi.org/10.1111/bre.12227

Morley, C. K., Tingay, M., Hillis, R., & King, R. (2008). Relationship between structural style, overpressures, and modern stress, Baram Delta province, Northwest Borneo. *Journal of Geophysical Research*, *113*(B09410), 1–23. https://doi.org/10.1029/2007JB005324

Murray, D. (2000). *Pohokura-1 well completion report*. New Zealand Petroleum Report Series No. 2491.

Neuzil, C. E., & Pollock, D. W. (1983). Erosional unloading and fluid pressures in hydraulically "tight" rocks. *The Journal of Geology*, *91*(2), 179–193. http://www.jstor.org/stable/30060924

NZP&M. (2018). *New Zealand petroleum exploration data pack*. https://data.nzpam.govt.nz/GOLD/system/mainframe.asp

O'Connor, S. A., & Swarbrick, R. E. (2008). Pressure regression, fluid drainage and a hydrodynamically controlled fluid contact in the North Sea, Lower Cretaceous, Britannia Sandstone Formation. *Petroleum Geoscience*, *14*(2), 115–126. https://doi.org/10.1144/1354-079308-737

O'Neill, S. R., Jones, S. J., Kamp, P. J. J., Swarbrick, R. E., & Gluyas, J. G. (2018). Pore pressure and reservoir quality evolution in the deep Taranaki Basin, New Zealand. *Marine and Petroleum Geology*, *98*(April), 815–835. https://doi.org/10.1016/J.MARPETGEO.2018.08.038

Osborne, M. J., & Swarbrick, R. E. (1997). Mechanisms for generating overpressure in sedimentary basins: A reevaluation. *American Association of Petroleum Geologists Bulletin*, *81*(6), 1023–1041. https://doi.org/10.1306/E4FD2D89-1732-11D7-8645000102C1865D

Prada, M., Lavoué, F., Saqab, M., O'Reilly, B., Lebedev, S., Walsh, J., & Childs, C. (2018). Across-axis variations in petrophysical properties of the North Porcupine Basin, offshore Ireland: new insights from long-streamer traveltime tomography. *Basin Research*, *31*, 59–76. https://doi.org/10.1111/bre.12308

Ramdhan, A. M., & Goulty, N. R. (2010). Overpressure-generating mechanisms in the Peciko field, lower Kutai Basin, Indonesia. *Petroleum Geoscience*, *16*(4), 367–376. https://doi.org/10.1144/1354-079309-027

Reilly, C., Nicol, A., Walsh, J. J., & Seebeck, H. (2015). Evolution of faulting and plate boundary deformation in the southern Taranaki Basin, New Zealand. *Tectonophysics*, *651*, 1–18. https://doi.org/10.1016/j.tecto.2015.02.009

Richards, F. W., Vrolijk, P. J., Gordon, J. D., & Miller, B. R. (2010). Reservoir connectivity analysis of a complex combination trap: Terra Nova field, Jeanne d'Arc Basin, Newfoundland, Canada. *Geological Society, London, Special Publications*, *347*(1), 333–355. https://doi.org/10.1144/SP347.19

Robertson, J., Goulty, N. R., & Swarbrick, R. E. (2013). Overpressure distributions in Palaeogene reservoirs of the UK Central North Sea and implications for lateral and vertical fluid flow. *Petroleum Geoscience*, *19*(3), 223–236. https://doi.org/10.1144/petgeo2012-060

Robertson, J. (2013). *Overpressure and lateral drainage in the palaeogene strata of the Central North Sea*. Durham University. http://etheses.dur.ac.uk/9452/

Roure, F., Andriessen, P., Callot, J. P., Faure, J. L., Ferket, H., Gonzales, E., Guilhamhou, N., Lacombe, O., Malandain, J., Sassi, W., Schneider, F., Sweneen, R., & Vilasi, N. (2010). The use of palaeo-thermo-barometers and coupled thermal, fluid flow and pore-fluid pressure modelling for hydrocarbon and reservoir prediction in fold and thrust belts. In G. P. Goffey, J. Craig, T. Needham, & R. Scott (Eds.), *Hydrocarbons in contractional belts* (pp. 87–114). Geological Society, London, Special Publications. https://doi.org/10.1144/SP348.6

Salazar, M., Moscardelli, L., & Wood, L. (2018). Two-dimensional stratigraphic forward modeling, reconstructing high-relief clinoforms in the northern Taranaki Basin. *AAPG Bulletin*, *102*(12), 2409–2446. https://doi.org/10.1306/04241817235

Sayers, C. M., Johnson, G. M., & Denyer, G. (2002). Predrill pore-pressure prediction using seismic data. *Geophysics*, *67*(4), 1286–1292. https://doi.org/10.1190/1.1500391

Sharman, G. R., Graham, S. A., Masalimova, L. U., Shumaker, L. E., & King, P. R. (2015). Spatial patterns of deformation and paleoslope estimation within the marginal and central portions of a basin-floor mass-transport deposit, Taranaki Basin, New Zealand. *Geosphere*, *11*(2), 266–306. https://doi.org/10.1130/GES01126.1

Shi, W., Xie, Y., Zhenfeng, W., Li, X., & Tong, C. (2013). Characteristics of overpressure distribution and its implication for hydrocarbon exploration in the Qiongdongnan Basin. *Journal of Asian Earth Sciences*, *66*, 150–165. https://doi.org/10.1016/j.jseaes.2012.12.037

Snell, T., De Paola, N., Van Hunen, J., Nielsen, S., & Collettini, C. (2019). Modelling fluid flow in complex natural fault zones: Implications for natural and human-induced earthquake nucleation. *Earth and Planetary Science Letters*, *530*, 115869. https://doi.org/10.1016/j.epsl.2019.115869

Stagpoole, V., & Funnell, R. (2001). Arc magmatism and hydrocarbon generation in the northern Taranaki Basin, New Zealand. *Petroleum Geoscience*, *7*(3), 255–267. https://doi.org/10.1144/petgeo.7.3.255

Stagpoole, V., Funnell, R., & Nicol, A. (2004). Overview of the structure and associated petroleum prospectivity of the Taranaki fault, New Zealand. *PESA Eastern Australian Basins Symposium II*, 197–206.

Stagpoole, V., & Nicol, A. (2008). Regional structure and kinematic history of a large subduction back thrust: Taranaki fault, New Zealand. *Journal of Geophysical Research: Solid Earth*, *113*(1), 1–19. https://doi.org/10.1029/2007JB005170

Stern, T. A., & Davey, F. J. (1990). Deep seismic expression of a foreland basin: Taranaki Basin, New Zealand. *Geology*, *18*(10), 979–982. https://doi.org/10.1130/0091-7613(1990)018<0979:DSEOAF>2.3.CO;2

Strogen, D. P. (2011). *Paleogeographic synthesis of the Taranaki Basin and surrounds*. GNS Science Report, 2010/53 (Issue June).

Strogen, D. P., Bland, K. J., Bull, S., Fohrmann, M. F., Scott, G. P. L., & Zhu, H. (2014). *Regional seismic transects of selected lines from Taranaki Basin*. GNS Data Series 7b.

Strogen, D. P., Bland, K. J., Nicol, A., & King, P. R. (2014). Paleogeography of the Taranaki Basin region during the latest Eocene-Early Miocene and implications for the total drowning of Zealandia. *New Zealand Journal of Geology and Geophysics*, *57*(2), 110–127. https://doi.org/10.1080/00288306.2014.901231

Strogen, D. P., Seebeck, H., Nicol, A., & King, P. R. (2017). Two-phase Cretaceous-Paleocene rifting in the Taranaki Basin region, New Zealand; implications for Gondwana break-up. *Journal of the Geological Society*, *174*(5), 929–946. https://doi.org/10.1144/jgs2016-160

Swarbrick, R. E., & Osborne, M. J. (1996). The nature and diversity of pressure transition zones. *Petroleum Geoscience*, *2*(2), 111–116. https://doi.org/10.1144/petgeo.2.2.111

Swarbrick, R. E., & Osborne, M. J. (1998). Mechanisms that generate abnormal pressures: An overview. In B. E. Law, G. F. Ulmishek, & V. I. Slavin (Eds.), *Abnormal pressures in hydrocarbon environments*. American Association of Petroleum Geologists. https://doi.org/10.1306/M70615C2

Swarbrick, R. E., Osborne, M. J., & Yardley, G. S. (2002). Comparison of overpressure magnitude resulting from the Main generating mechanisms. In A. R. Huffman & G. L. Bowers (Eds.), *Pressure regimes in sedimentary basins and their prediction* (Vol. *76*, pp. 1–12). AAPG Memoir.

Tingay, M. R. P., Hillis, R. R., Morley, C. K., Swarbrick, R. E., & Drake, S. J. (2005). Present-day stress orientation in Brunei: A snapshot of 'prograding tectonics' in a tertiary delta. *Journal of the Geological Society*, *162*(1), 39–49. http://jgs.lyellcollection.org/content/162/1/39.abstract

Tingay, M. R. P., Hillis, R. R., Swarbrick, R. E., Morley, C. K., & Damit, A. R. (2007). Vertically transferred' overpressures in Brunei: Evidence for a new mechanism for the formation of high-magnitude overpressure. *Geology*, *35*(11), 1023. https://doi.org/10.1130/G23906A.1

Tingay, M. R. P., Morley, C. K., Laird, A., Limpornpipat, O., Krisadasima, K., Pabchanda, S., & Macintyre, H. R. (2013). Evidence for overpressure generation by kerogen-to-gas maturation in the northern Malay Basin. *AAPG Bulletin*, *97*(4), 639–672. https://doi.org/10.1306/09041212032

Tippett, J. M., & Kamp, P. J. J. (1993). Fission track analysis of the Late Cenozoic vertical kinematics of continental pacific crust, South Island, New Zealand. *Journal of Geophysical Research: Solid Earth*, *98*(B9), 16119–16148.

Traugott, M. (1997). Pore/fracture pressure determinations in deep water. *Pipe Line and Gas Industry*.

Tripathi, A. R. P., & Kamp, P. J. J. (2008). Timing of initiation of reverse displacement on the Taranaki Fault, northern Taranaki Basin: Constraints from the on land record (Oligocene Te Kuiti Group). *Proceedings of 2008 New Zealand Petroleum Conference, Auckland, New Zealand, 9–12 March 2008*, 1–17.

Van Balen, R., & Cloetingh, S. (1994). Tectonic control of the sedimentary record and stress-induced fluid flow: Constraints from basin modelling. *Geological Society, London, Special Publications*, *78*(1), 9–26.

van Ruth, P., Hillis, R., Swarbrick, R., & Tingate, P. (2000). Mud weights, transient pressure tests, and the distribution of overpressure in the north west shelf, Australia. *Petroleum Exploration Society of Australia (PESEA) Journal*, *28*, 59–66.

Voggenreiter, W. R. (1993). Structure and evolution of the Kapuni Anticline, Taranaki Basin, New Zealand: Evidence from the Kapuni 3D seismic survey. *New Zealand Journal of Geology and Geophysics*, *36*(May), 77–94. https://doi.org/10.1080/00288306.1993.9514556

Wallace, L. M., Kaneko, Y., Hreinsdóttir, S., Hamling, I., Peng, Z., Bartlow, N., Anastasio, E. D., & Fry, B. (2017). Slip enhanced by overlying sedimentary wedge. *Nature Geoscience*, *10*, 765–770. https://doi.org/10.1038/NGEO3021

Webster, M., O'Connor, S., Pindar, B., & Swarbrick, R. (2011). Overpressures in the Taranaki Basin: Distribution, causes, and implications for exploration. *AAPG Bulletin*, *95*(3), 339–370. https://doi.org/10.1306/06301009149

Williamson, M. A. (1995). Overpressures and hydrocarbon generation in the sable sub-basin, offshore Nova Scotia. *Basin Research*, *7*(1), 21–34. https://doi.org/10.1111/j.1365-2117.1995.tb00092.x

Wonham, J. P., Cyrot, M., Nguyen, T., Louhouamou, J., & Ruau, O. (2010). Integrated approach to geomodelling and dynamic simulation in a complex mixed siliciclastic-carbonate reservoir, N'Kossa field, offshore Congo. *Geological Society, London, Special Publications*, *347*(1), 133–163. https://doi.org/10.1144/sp347.10

Xie, X., Bethke, C. M., Li, S., Liu, X., & Zheng, H. (2001). Overpressure and petroleum generation and accumulation in the Dongying depression of the Bohaiwan Basin, China. *Geofluids*, *1*(4), 257–271. https://doi.org/10.1046/j.1468-8123.2001.00017.x

Yan, S., Xinyu, X., Feng, H., Shengfei, Q., & Guoyou, F. U. (2002). Abnormal overpressure distribution and natural gas accumulation in foreland basins, Western China. *Chinese Science Bulletin*, *47*, 71–77.

Yardley, G. S., & Swarbrick, R. E. (2000). Lateral transfer: A source of additional overpressure? *Marine and Petroleum Geology*, *17*(4), 523–537. https://doi.org/10.1016/S0264-8172(00)00007-6

Zhang, J. (2011). Pore pressure prediction from well logs: Methods, modifications, and new approaches. *Earth-Science Reviews*, *108*(1–2), 50–63. https://doi.org/10.1016/j.earscirev.2011.06.001

Zoccarato, C., Minderhoud, P. S. J., & Teatini, P. (2018). The role of sedimentation and natural compaction in a prograding delta: Insights from the mega Mekong delta, Vietnam. *Scientific Reports*, *8*(1), 1–12. https://doi.org/10.1038/s41598-018-29734-7

SUPPORTING INFORMATION

Additional supporting information can be found online in the Supporting Information section at the end of this article.

How to cite this article: O'Neill, S. R., Jones, S. J., & Kamp, P. J. J. (2023). Tectonostratigraphic controls on pore fluid pressure distribution across the Taranaki Basin, New Zealand. *Basin Research*, *00*, 1–26. https://doi.org/10.1111/bre.12749